Cognitive Network Interference

Alberto Rabbachin, *Member, IEEE*, Tony Q.S. Quek, *Member, IEEE*, Hyundong Shin, *Member, IEEE*, and Moe Z. Win, *Fellow, IEEE*

***Abstract*—Opportunistic spectrum access creates the opening of under-utilized portions of the licensed spectrum for reuse, provided that the transmissions of secondary radios do not cause harmful interference to primary users. Such a system would require secondary users to be cognitive—they must accurately detect and rapidly react to varying spectrum usage. Therefore, it is important to characterize the effect of cognitive network interference due to such secondary spectrum reuse. In this paper, we propose a new statistical model for aggregate interference of a cognitive network, which accounts for the sensing procedure, secondary spatial reuse protocol, and environment-dependent conditions such as path loss, shadowing, and channel fading. We first derive the characteristic function and cumulants of the cognitive network interference at a primary user. Using the theory of truncated-stable distributions, we then develop the statistical model for the cognitive network interference. We further extend this model to include the effect of power control and demonstrate the use of our model in evaluating the system performance of cognitive networks. Numerical results show the effectiveness of our model for capturing the statistical behavior of the cognitive network interference. This work provides essential understanding of interference for successful deployment of future cognitive networks.**

***Index Terms*—Opportunistic spectrum access, cognitive radio, cognitive network interference, detection-and-avoidance, truncated-stable distribution.**

I. INTRODUCTION

WITH the emergence of new wireless applications and devices, there is a dramatic increase in the demand for radio spectrum. Due to the scarcity of radio spectrum and the under-utilization of assigned spectrum, government regulatory bodies such as the U.S. Federal Communications Commission (FCC) have started to review their spectrum allocation policies [1], [2]. Conventional rigid spectrum allocation forbids flexible spectrum usage that severely hinders efficient utilization of scarce spectrum since bandwidth demands vary along time and space dimensions. Therefore, opportunistic spectrum access together with a cognitive radio (CR) technology has become a promising solution to resolve this problem [3]–[7].

Opportunistic spectrum access creates the opening of under-utilized portions of the licensed spectrum for reuse, provided that the transmissions of secondary radios do not cause harmful interference to primary users. For secondary users to accurately detect and access the idle spectrum, CR has been proposed as an enabling technology [3], [4], [7]. For example, if a communication channel is active between the primary and secondary networks, the busy channel assessment can be based on the detection of a preamble shared between the primary and secondary networks or on the energy sensing of the primary network radio signals [8]–[10]. Moreover, the CR network can implement a detect-and-avoid protocol where the transmission power levels of the CR devices are based on the sensed power of the primary network signals.

Spectrum sharing is however challenging due to the uncertainty associated with the aggregate interference in the network. Such uncertainty can be resulted from the unknown number of interferers and unknown locations of the interferers as well as channel fading, shadowing, and other uncertain environment-dependent conditions [11], [12]. Therefore, it is crucial to incorporate such uncertainty in the statistical interference model in order to quantify the effect of the *cognitive network interference* on the primary network system performance.[1] A unifying framework for characterizing the network interference was proposed to investigate a variety of issues involving aggregate interference generated asynchronously in a wireless environment subject to path loss, shadowing, and multipath fading [13], [14]. The original motivation for this work was to quantify the aggregate network emission of randomly located ultra-wide bandwidth (UWB) radios [15]–[17] in terms of their spatial density [18]–[20]. This framework has also been used to study the coexistence issues in heterogeneous wireless networks [21]–[25]. A common theme of all these work is the use of a Poisson point process [26] for positions of the emitting nodes. The Poisson point process has been widely used in diverse fields such as astronomy [27], [28], positron emission tomography [29], cell biology [30], optical communications [31]–[34], and wireless communications [28], [35]–[40]. More recently, the Poisson model has been applied for spatial node distributions in a variety of wireless networks such as random access, ad hoc, relay, cognitive radio, or femtocell networks [41]–[52].

To address the coexistence problem arisen by secondary

Manuscript received 1 December 2009; revised 30 May 2010. This research was supported, in part, by the MIT Institute for Soldier Nanotechnologies, the Office of Naval Research Presidential Early Career Award for Scientists and Engineers (PECASE) N00014-09-1-0435, and the National Science Foundation under grant ECCS-0901034, and the National Research Foundation of Korea (KRF) grant funded by the Korea government (MEST) (No. 2010-0014773).

A. Rabbachin is with the Institute for the Protection and Security of the Citizen of the Joint Research Center, European Commission, 21027 Ispra, Italy (e-mail: alberto.rabbachin@jrc.ec.europa.eu).

T. Q. S. Quek is with the Institute for Infocomm Research, A*STAR, 1 Fusionopolis Way, #21-01 Connexis South Tower, Singapore 138632 (e-mail: qsquek@ieee.org).

H. Shin is with the Department of Electronics and Radio Engineering, Kyung Hee University, 1 Seocheon-dong, Giheung-gu, Yongin-si, Gyeonggi-do, 446-701 Korea (e-mail: hshin@khu.ac.kr).

M. Z. Win is with the Laboratory for Information & Decision Systems (LIDS), Massachusetts Institute of Technology, 77 Massachusetts Avenue, Cambridge, MA 02139 (e-mail: moewin@mit.edu).

Digital Object Identifier 10.1109/JSAC.2011.110219.

[1]Throughout this paper, we refer to the aggregate interference generated by secondary users sharing the same spectrum with the primary user as cognitive network interference.

cognitive networks, it is of great importance to accurately model the aggregate interference generated by multiple active secondary users in the network. In [48], the moment expression for the aggregate interference generated by Poisson nodes in an arbitrary area was derived assuming the typical unbounded path-loss model. However, the unbounded path-loss model results in significant deviations from a realistic performance [49]. For cognitive radio networks, the log-normal distribution was proposed to model the sum of all interferers' powers [45]. This log-normal approximation was also used for the aggregate interference at primary users without accounting for the channel uncertainty due to fading [46]. The optimal power control strategies for secondary users were determined in [47] based on the Poisson model of the primary network.

In this paper, we propose a new statistical model for *per-dimension* (real or imaginary part) aggregate interference of a cognitive network, accounting for the sensing procedure, secondary spatial reuse protocol, spatial density of the secondary users and environment-dependent conditions such as path loss, shadowing, and channel fading. Moreover, our framework allows us to model the cognitive network interference generated by secondary users in a *limited* or *finite* region, taking into account the shape of the region and the position of the primary user. As an example, we consider two types of secondary spatial reuse protocols, namely, single-threshold and multiple-threshold protocols. For each protocol, we first express the characteristic function (CF) of the cognitive network interference, from which we derive its cumulants. Using these cumulants, we then model the cognitive network interference as truncated-stable random variables. We further extend this model to include the effect of power control and demonstrate the use of our model in evaluating a system performance such as the bit error probability (BEP) in the presence of cognitive network interference. Numerical results verify the validity of our model in capturing the effect of the cognitive network interference in different scenarios.

The paper is organized as follows. Section II presents the system model. Section III derives the instantaneous interference distribution and its truncated-stable model for each secondary spatial reuse protocol. Section IV demonstrates applications of our statistical model for cognitive network interference. Section V provides numerical results to illustrate the effectiveness of our framework for characterizing the coexistence between primary and secondary networks in terms of various system parameters. Section VI gives the conclusion. We relegate the glossary of statistical symbols used throughout the paper to Appendix A and the derivations of cumulants to Appendix B.

II. System Model

For cognitive networks, the secondary users need to sense channels before transmission in order not to cause harmful interference to a primary network. In this paper, we consider the primary network in frequency division duplex mode. Therefore, to detect the presence of active primary users, the secondary user senses the primary users' uplink channel. Furthermore, we consider the secondary network as a simple *ad-hoc* network where secondary users join or exit the network, and sense or access the channel independently without coordinating with other secondary users [53]–[55]. As such, there exists the possibility that secondary users can transmit at the same time regardless of their distances between each other.[2]

A. Cognitive Network Activity Model

The activity of each secondary user depends on the strength of the received uplink signal transmitted by the primary user. In the following, we consider two types of secondary spatial reuse protocols, namely: single-threshold and multiple-threshold protocols.

1) Single-Threshold Protocol: In this case, the ith secondary user is active if

$$\frac{K P_{\mathrm{p}} Y_i}{R_i^{2b}} \leq \beta, \tag{1}$$

or equivalently,

$$R_i^{-2b} Y_i \leq \zeta, \tag{2}$$

where β is the activating threshold; $\zeta \triangleq \frac{\beta}{K P_{\mathrm{p}}}$ is the *normalized* threshold; P_{p} is the transmitted power of the primary user; Y_i is the squared fading path gain of the channel from the primary user to the ith secondary user; K is the gain accounting for the loss in the near-field; R_i is the distance between the primary and the ith secondary user; and b is the amplitude pass-loss exponent.[3] We assume that Y_i's are independent and identically distributed (IID) with the common cumulative distribution function (CDF) $F_Y(\cdot)$. Therefore, the activity of the secondary network users can be represented by the Bernoulli random variable:

$$\mathbb{1}_{[0,\zeta]}\left(R_i^{-2b} Y_i\right) \sim \mathsf{Bern}\left(F_{Y_i}\left(R_i^{2b}\zeta\right)\right), \tag{3}$$

with the indicator function defined as

$$\mathbb{1}_{[p,q]}(x) = \begin{cases} 1, & \text{if } p \leq x \leq q, \\ 0, & \text{otherwise,} \end{cases} \tag{4}$$

where the value one of the Bernoulli variable denotes that the secondary user is active.

2) Multiple-Threshold Protocol: For this case, the transmission power of the secondary network users is set according to the detected power level of the primary network uplink signal [56]. We consider $N-1$ normalized threshold values $\zeta_1, \zeta_2, \ldots, \zeta_{N-1}$ in increasing order to identify N different classes (or sets) of active secondary users, denoted by $\mathcal{A}_k$, $k = 1, 2, \ldots, N$. Let $\zeta_0 = 0$ and $\zeta_N = \infty$. Then, the kth active class $\mathcal{A}_k$ obeys the following activation rule:[4]

$$\mathbb{1}_{[\zeta_{k-1},\zeta_k]}\left(R_i^{-2b} Y_i\right) \sim \mathsf{Bern}\left(\mu_{Y_i}^{(\mathrm{pt})}\left(0, R_i^{2b}\zeta_{k-1}, R_i^{2b}\zeta_k\right)\right). \tag{5}$$

[2]When a more intelligent medium access control protocol that involves a form of coordination or local information exchange is feasible for the secondary network, our results can still serve as a worst-case scenario analysis.

[3]For brevity, we assume that the noise effect is negligible on the primary detection procedure as in [45].

[4]The zeroth-order partial moment $\mu_X^{(\mathrm{pt})}(0, l, u)$ of the random variable X can be written in terms of its CDF as

$$\mu_X^{(\mathrm{pt})}(0, l, u) = F_X(u) - F_X(l).$$

Note that the power of the received primary user's signal at the active secondary users in the class $\mathcal{A}_k$ is between $KP_{\mathrm{p}}\zeta_{k-1}$ and $KP_{\mathrm{p}}\zeta_k$.

B. Interference Model

The interference signal at the primary receiver generated by the ith cognitive interferer can be written as

$$I_i = \sqrt{P_{\mathrm{I}}} R_i^{-b} X_i, \tag{6}$$

where P_{I} is the interference signal power at the limit of the near-far region;[5] R_i is the distance between the ith cognitive interferer and the primary receiver; and X_i is the *per-dimension* fading channel path gain of the channel from the ith cognitive interferer to the primary receiver.[6] In the following, we assume that X_i's are IID with the common probability density function (PDF) $f_X(\cdot)$, which are mutually independent of Y_i's.

We consider that the secondary users are spatially scattered according to an homogeneous Poisson point process in a two-dimensional plane $\mathbb{R}^2$, where the victim primary user is assumed to be located at the center of the region. Let $\mathcal{S} \subset \mathbb{Z}^+$ be the index set of secondary users in a region $\mathcal{R} \subset \mathbb{R}^2$. Then the probability that k secondary users lie inside $\mathcal{R}$ depends only on the total area $A_{\mathcal{R}}$ of the region, and is given by [26]

$$\mathbb{P}\left\{|\mathcal{S}| = k\right\} = \frac{(\lambda A_{\mathcal{R}})^k}{k!} e^{-\lambda A_{\mathcal{R}}}, \quad k = 0, 1, 2, \ldots \tag{7}$$

where λ is the spatial density (in nodes per unit area). Furthermore, we assume that the region $\mathcal{R}$ is constrained in the annulus prescribed by two radius $d_{\min}$ and $d_{\max}$, which are minimum and maximum distances from the primary receiver, respectively.[7] This allows us to consider a scenario where the secondary users are located within a limited region.

III. Instantaneous Interference Distribution

To characterize the cognitive network interference, we first derive the cumulants for the cases of full network activity (all secondary users are active) and regulated activity (each secondary user is regulated by a spatial reuse protocol) in Section III-A and III-B, respectively. Using these cumulant expressions, we develop the symmetric truncated-stable model for the cognitive network interference in Section III-C.

A. Full Activity

In this case, the cognitive network interference is generated by all the secondary users present in the region $\mathcal{R}$ and can be written as

$$I_{\mathrm{fa}} = \sqrt{P_{\mathrm{I}}} \underbrace{\sum_{i \in \mathcal{S}} R_i^{-b} X_i}_{Z_{\mathrm{fa}}(\mathcal{R})}. \tag{8}$$

By using [14, Theorem 3.1], the CF of $Z_{\mathrm{fa}}(\mathcal{R})$ can be expressed as

$$\psi_{Z_{\mathrm{fa}}(\mathcal{R})}(j\omega) = \exp\left(-2\pi\lambda \int_X \int_{d_{\min}}^{d_{\max}} \left[1 - \exp\left(j\omega x r^{-b}\right)\right] \times f_X(x)\, r dr dx\right), \tag{9}$$

where $j = \sqrt{-1}$. Using (9), we can then calculate the nth cumulant of the interference $Z_{\mathrm{fa}}(\mathcal{R})$ as follows:

$$\begin{aligned} \kappa_{Z_{\mathrm{fa}}(\mathcal{R})}(n) &= \frac{1}{j^n} \frac{d^n \ln \psi_{Z_{\mathrm{fa}}(\mathcal{R})}(j\omega)}{d\omega^n}\bigg|_{\omega=0} \\ &= 2\pi\lambda \int_X \int_{d_{\min}}^{d_{\max}} x^n r^{1-nb} f_X(x)\, dr dx \\ &= \frac{2\pi\lambda}{nb-2}\left(d_{\min}^{2-nb} - d_{\max}^{2-nb}\right) \mu_X(n). \end{aligned} \tag{10}$$

Using the cumulant of $Z_{\mathrm{fa}}(\mathcal{R})$, we can obtain the nth cumulant of the cognitive network interference I_{fa} for the full activity case as follows:

$$\kappa_{I_{\mathrm{fa}}}(n) = P_{\mathrm{I}}^{n/2} \kappa_{Z_{\mathrm{fa}}(\mathcal{R})}(n). \tag{11}$$

B. Regulated Activity

1) Single-Threshold Protocol: In this spatial reuse protocol, the activity of the secondary users in the region $\mathcal{R}$ is regulated by the single normalized threshold ζ according to (3). Therefore, the cognitive network interference for the single-threshold protocol can be written as

$$I_{\mathrm{st}} = \sqrt{P_{\mathrm{I}}} \underbrace{\sum_{i \in \mathcal{A}_{\mathrm{st}}} R_i^{-b} X_i}_{Z_{\mathrm{st}}(\zeta;\mathcal{R})}, \tag{12}$$

where $\mathcal{A}_{\mathrm{st}}$ defines the index set of active secondary users in the region $\mathcal{R}$:

$$\mathcal{A}_{\mathrm{st}} = \left\{i \in \mathcal{S} : \mathbb{1}_{[0,\zeta]}\left(R_i^{-2b} Y_i\right) = 1\right\}. \tag{13}$$

Similar to (9), the CF of $Z_{\mathrm{st}}(\zeta;\mathcal{R})$ can be expressed as

$$\begin{aligned} &\psi_{Z_{\mathrm{st}}(\zeta;\mathcal{R})}(j\omega) \\ &= \exp\left(-2\pi\lambda \int_X \int_Y \int_{d_{\min}}^{d_{\max}} \left[1 - \exp\left(j\omega x r^{-b}\right)\right] \times \mathbb{1}_{[0,\zeta]}\left(r^{-2b} y\right) f_X(x) f_Y(y)\, r dr dy dx\right), \end{aligned} \tag{14}$$

from which the cumulant $\kappa_{Z_{\mathrm{st}}(\zeta;\mathcal{R})}(n)$ is derived in Appendix B-A. Using the cumulant of $Z_{\mathrm{st}}(\zeta;\mathcal{R})$, we can obtain the nth cumulant of the cognitive network interference I_{st} for the single-threshold protocol as follows:

$$\kappa_{I_{\mathrm{st}}}(n) = P_{\mathrm{I}}^{n/2} \kappa_{Z_{\mathrm{st}}(\zeta;\mathcal{R})}(n). \tag{15}$$

Remark 1: As $\zeta \to \infty$, the second and third terms in (38) vanish and hence,

$$\lim_{\zeta \to \infty} \kappa_{I_{\mathrm{st}}}(n) = \kappa_{I_{\mathrm{fa}}}(n), \tag{16}$$

as expected. Therefore, the full activity can be viewed as an extreme case of the single-threshold spatial reuse such that $\zeta \to \infty$.

[5] We consider the near-far region limit at 1 meter.

[6] Note that $X_i = \Re\{H_i\}$, where H_i is the complex path gain of the channel from the ith cognitive interferer to the primary receiver.

[7] Note that R_i in (6) can be smaller than 1. Therefore, the received interference power can be larger than P_{I} but it is finite since $d_{\min} > 0$.

2) Multiple-Threshold Protocol: Using (5), the per-class cognitive interference generated by the secondary users in $\mathcal{A}_k$ can be written as

$$I_{\mathrm{mt},k} = \sqrt{P_{\mathrm{I},k}} \underbrace{\sum_{i \in \mathcal{A}_k} R_i^{-b} X_i}_{Z_k(\mathcal{R})}, \tag{17}$$

where $P_{\mathrm{I},k}$ is the transmitted power of the secondary users in the kth active class $\mathcal{A}_k$ and

$$\mathcal{A}_k = \left\{ i \in \mathcal{S} : \mathbb{1}_{[\zeta_{k-1},\zeta_k]} \left(R_i^{-2b} Y_i \right) = 1 \right\}. \tag{18}$$

The N power levels $P_{\mathrm{I},1}, P_{\mathrm{I},2}, \ldots, P_{\mathrm{I},N}$ are set in decreasing order such that users active in classes characterized by higher detected power level of the primary signal transmit with lower power. Similar to (14), the CF of $Z_k(\mathcal{R})$ can be expressed as

$$\psi_{Z_k(\mathcal{R})}(j\omega) = \exp\Bigg(-2\pi\lambda \int_X \int_Y \int_{d_{\min}}^{d_{\max}} \left[1 - \exp\left(j\omega x r^{-b} \right) \right] \times \mathbb{1}_{[\zeta_{k-1},\zeta_k]} \left(r^{-2b} y \right) f_X(x) f_Y(y)\, r dr dy dx \Bigg). \tag{19}$$

The cognitive network interference generated by the secondary users in all the N classes is then given by

$$I_{\mathrm{mt}} = \sum_{k=1}^{N} \sqrt{P_{\mathrm{I},k}} Z_k(\mathcal{R}). \tag{20}$$

Since all the $Z_k(\mathcal{R})$'s are statistically independent,[8] we obtain the nth cumulant of the cognitive network interference I_{mt} for the multiple-threshold protocol as

$$\kappa_{I_{\mathrm{mt}}}(n) = \sum_{k=1}^{N} P_{\mathrm{I},k}^{n/2} \kappa_{Z_k(\mathcal{R})}(n), \tag{21}$$

where $\kappa_{Z_k(\mathcal{R})}(n)$ are given by (40), (44), and (46) in Appendix B-B for $k = 1$, $k = 2, 3, \ldots, N-1$, and $k = N$, respectively.

Remark 2: Using the cumulant expressions (10), (15), and (21), we can characterize statistical properties (e.g., mean, variance, and other higher order statistics) of the cognitive network interference for each secondary spatial reuse protocol. For example, the second-order cumulant can be used to measure the power of the cognitive network interference.

C. Truncated-Stable Distribution Model

The truncated-stable distributions are a relatively new class of distributions that follow from the class of stable distributions [57]. The attractivenesses of using stable distributions to model interference in wireless networks are: 1) the ability to capture the spatial distribution of the interfering nodes; and 2) the ability to accommodate heavy tail behavior exhibiting the dominant contribution of a few interferers in the vicinity of the primary user [58]. However, as shown in [14], the aggregate interference converges to a stable distribution only if the interferers are scattered in the entire plane. Stable distributions have unbounded (infinite) second-order moment due to the singularity at $r = 0$ and thus, care must be taken when using this model. The truncated-stable distributions have smoothed tails and finite moments, offering an alternative statistical tool to model the aggregate interference in more realistic scenarios without this singularity.

The CF of a symmetric truncated-stable random variable $T \sim \mathcal{S}_{\mathrm{t}}(\gamma', \alpha, g)$ is given by [59]

$$\psi_T(j\omega) = \exp\left(\gamma' \Gamma(-\alpha) \left[\frac{(g - j\omega)^{\alpha}}{2} + \frac{(g + j\omega)^{\alpha}}{2} - g^{\alpha} \right] \right), \tag{22}$$

where $\Gamma(\cdot)$ is the Euler's gamma function; and γ', α and g are the parameters associated with the truncated-stable distribution. The parameters γ' and α are akin to the dispersion and the characteristic exponent of the stable distribution, respectively. The parameter g is the argument of the exponential function used to smooth the tail of the stable distribution. The nth cumulant of the truncated-stable distribution can be obtained using (22) as

$$\kappa_T(n) = \begin{cases} \gamma' \Gamma(-\alpha)\, g^{\alpha - n} \prod_{i=0}^{n-1} (\alpha - i), & \text{for even } n \\ 0, & \text{for odd } n. \end{cases} \tag{23}$$

For given α, using (23), the parameters γ' and g can be expressed in terms of the first two nonzero cumulants, namely, the second- and fourth-order cumulants.

To model the cognitive network interference using the truncated-stable distribution, we first fix the characteristic exponent to $\alpha = 2/b$. This choice is motivated by the fact that as $d_{\min} \to 0$ and $d_{\max} \to \infty$, the cognitive network interference follows a stable distribution with the characteristic exponent $\alpha = 2/b$. Let I_{A} be the cognitive network interference corresponding to the activity model $\mathrm{A} \in \{\mathrm{fa}, \mathrm{st}, \mathrm{mt}\}$, i.e., full activity, regulated activity with the single-threshold protocol, or the multiple-threshold protocol. Then, we can model the cognitive network interference I_{A} as the symmetric truncated-stable random variable, i.e.,

$$I_{\mathrm{A}} \sim \mathcal{S}_{\mathrm{t}}\left(\gamma'_{\mathrm{A}}, \alpha = 2/b, g_{\mathrm{A}} \right), \tag{24}$$

where the dispersion and smoothing parameters γ'_{A} and g_{A} are given in terms of the second and fourth cumulants of I_{A} as

$$\gamma'_{\mathrm{A}} = \frac{\kappa_{I_{\mathrm{A}}}(2)}{\Gamma(-\alpha)\, \alpha (\alpha - 1) \left[\frac{\kappa_{I_{\mathrm{A}}}(2)(\alpha-2)(\alpha-3)}{\kappa_{I_{\mathrm{A}}}(4)} \right]^{\frac{\alpha-2}{2}}}, \tag{25}$$

$$g_{\mathrm{A}} = \sqrt{\frac{\kappa_{I_{\mathrm{A}}}(2)(\alpha - 2)(\alpha - 3)}{\kappa_{I_{\mathrm{A}}}(4)}}. \tag{26}$$

To validate our statistical model, we consider an annulus region defined by $d_{\min} = 1$ meter, $d_{\max} = 60$ meters, and $\lambda = 0.1$ users/m^2. Both primary and secondary signals experience Rayleigh fading, i.e., $\sqrt{Y_i} \sim \mathrm{Rayleigh}(1/2)$ and $|H_i| \sim \mathrm{Rayleigh}(1/2)$. We consider the multiple-threshold

[8] The cumulants have the linear property for independent random variables, i.e., if X and Y are independent, then

$$\kappa_{X+Y}(n) = \kappa_X(n) + \kappa_Y(n).$$

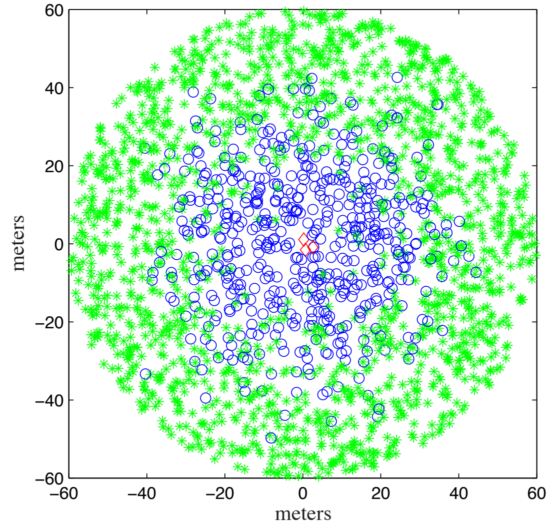

Fig. 1. Node displacements of a CR network with the multiple-threshold protocol (not only a single realization snapshot). $d_{\min} = 1$ meter, $d_{\max} = 60$ meters, $\lambda = 0.1$ users$/m^2$, $N = 3$, $\zeta_1 = -42$ dBm, and $\zeta_2 = -20$ dBm. The green (asterisk), blue (circle), and red (diamond) colors (markers) represent the classes $\mathcal{A}_1$, $\mathcal{A}_2$, and $\mathcal{A}_3$, respectively.

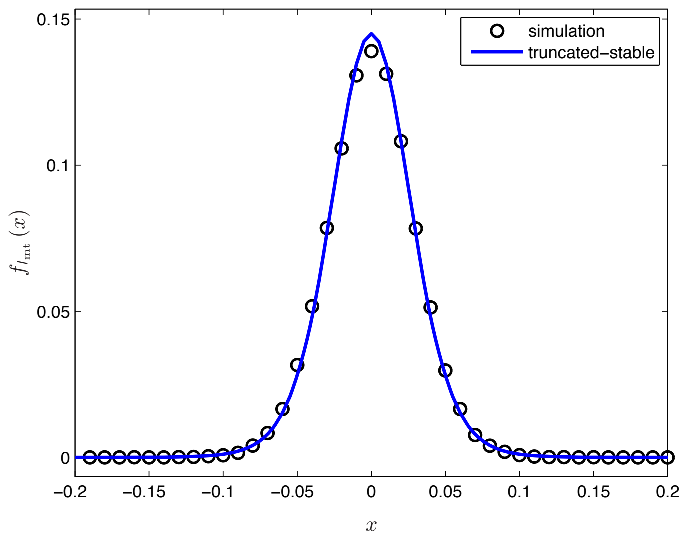

Fig. 2. PDF of the cognitive network interference $I_{\rm mt}$ for the multiple-threshold protocol with the same parameters as in Fig. 1. $P_{\rm I,1} = 0$ dBm for $\mathcal{A}_1$, $P_{\rm I,2} = -23.7$ dBm for $\mathcal{A}_2$, and $P_{\rm I,3} = -38.7$ dBm for $\mathcal{A}_3$.

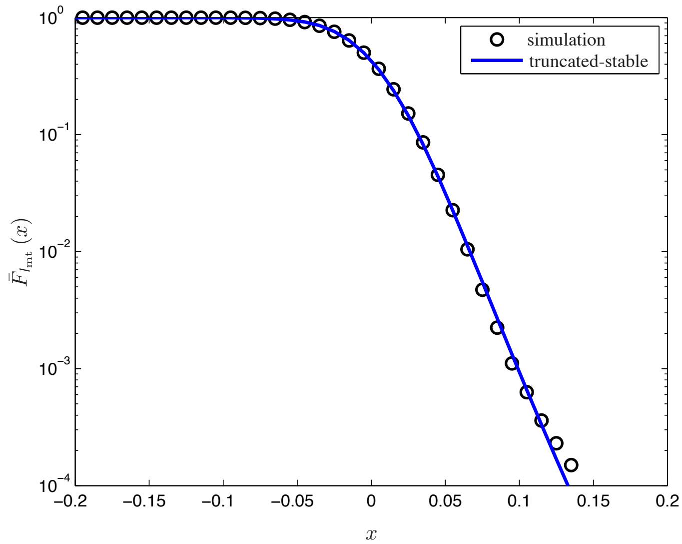

Fig. 3. CCDF of the cognitive network interference $I_{\rm mt}$ for the multiple-threshold protocol with the same parameters as in Fig. 1. $P_{\rm I,1} = 0$ dBm for $\mathcal{A}_1$, $P_{\rm I,2} = -23.7$ dBm for $\mathcal{A}_2$, and $P_{\rm I,3} = -38.7$ dBm for $\mathcal{A}_3$.

protocol implemented using two thresholds (i.e., $N = 3$) with the following parameters: the secondary network users transmit with power $P_{\rm I,1} = 0$ dBm if the signal power coming from the primary user is lower than $\zeta_1 = -42$ dBm, with power $P_{\rm I,2} = -23.7$ dBm if the signal power coming from the primary user is between ζ_1 and $\zeta_2 = -20$ dBm, and with power $P_{\rm I,3} = -38.7$ dBm if the signal power coming from the primary user is higher than ζ_2. Fig. 1 shows realization snapshots of active secondary users regulated by this multiple-threshold protocol, while Figs. 2 and 3 show the PDF and complementary CDF (CCDF) of the cognitive network interference $I_{\rm mt}$. We can observe from Figs. 2 and 3 that the simulation results match well with the truncated-stable statistical model.

With the symmetric truncated-stable model, we can also account for shadowing in the characterization of the cognitive network interference. For example, consider the single-threshold protocol shadowing environment with obstacles such that the whole region $\mathcal{R}$ can be divided into different subregions $\mathcal{R}_0$, and $\mathcal{R}_1, \mathcal{R}_2, \ldots, \mathcal{R}_L$ corresponding to the positions of the obstacles. Due to shadowing, these L subregions experience additional attenuation behind those obstacles. Then, the cognitive network interference can be written as

$$I_{\rm st} = \sum_{\ell=0}^{L} \sqrt{P_{{\rm I},\ell}} \underbrace{\sum_{i \in \mathcal{A}_{{\rm st},\ell}} R_i^{-b} X_i}_{Z_{\rm st}(\zeta\breve{\beta}_\ell;\mathcal{R}_\ell)}, \tag{27}$$

where

$$\mathcal{A}_{{\rm st},\ell} = \left\{ i \in \mathcal{S} \cap \mathcal{R}_\ell : \mathbb{1}_{[0,\zeta\breve{\beta}_\ell]}\left(R_i^{-2b} Y_i\right) = 1 \right\}. \tag{28}$$

For $\ell = 1, 2, \ldots, L$, $P_{{\rm I},\ell}$ and $\breve{\beta}_\ell$ account for an additional attenuation for the subregion $\mathcal{R}_\ell$ behind the obstacle, and $P_{\rm I,0} = P_{\rm I}$ and $\breve{\beta}_0 = 1$. The CF of $Z_{\rm st}(\zeta\breve{\beta}_\ell;\mathcal{R}_\ell)$ can be expressed as

$$\psi_{Z_{\rm st}(\zeta\breve{\beta}_\ell;\mathcal{R}_\ell)}(j\omega) = \exp\Bigg(-\theta_\ell \lambda \int_X \int_Y \int_{a_\ell}^{b_\ell} \left[1 - \exp\left(j\omega x r^{-b}\right)\right] \times \mathbb{1}_{[0,\zeta\breve{\beta}_\ell]}\left(r^{-2b} y\right) f_X(x) f_Y(y)\, r dr dy dx \Bigg). \tag{29}$$

where a_ℓ and b_ℓ are the limits of the subregion $\mathcal{R}_\ell$; and θ_ℓ is the angle covered by $\mathcal{R}_\ell$. If the obstacle is present, the angle θ_ℓ corresponds to the angle covered by the obstacle. For a single obstacle placed at distance d from the origin, we have two subregions in front and behind the obstacle:

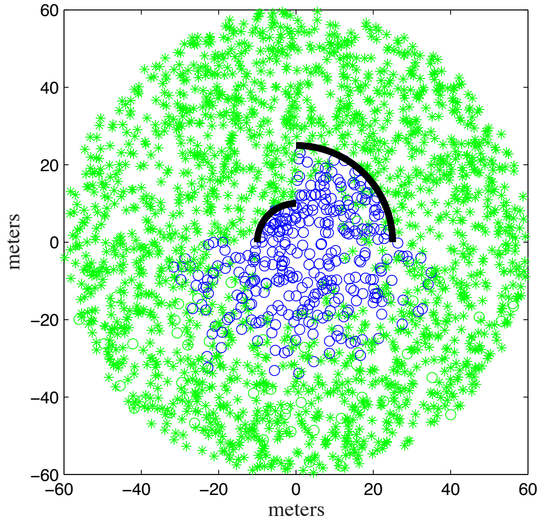

Fig. 4. Node displacements of a CR network with the single-threshold protocol in the presence of shadowing (not only a single realization snapshot). $d_{\min} = 1$ meter, $d_{\max} = 60$ meters, $\lambda = 0.01$ users$/m^2$, $\zeta = -40$ dBm, $\theta_1 = \theta_2 = \pi/2$, and $\breve{\beta}_1 = \breve{\beta}_2 = 20$ dB. The shadowing is characterized by two obstacles present at 10 and 25 meters from the primary receiver, covering the angle of $\pi/2$, and causing additional attenuation of 20 dB. The blue (circle) and green (asterisks) colors (markers) represent inactive and active nodes, respectively.

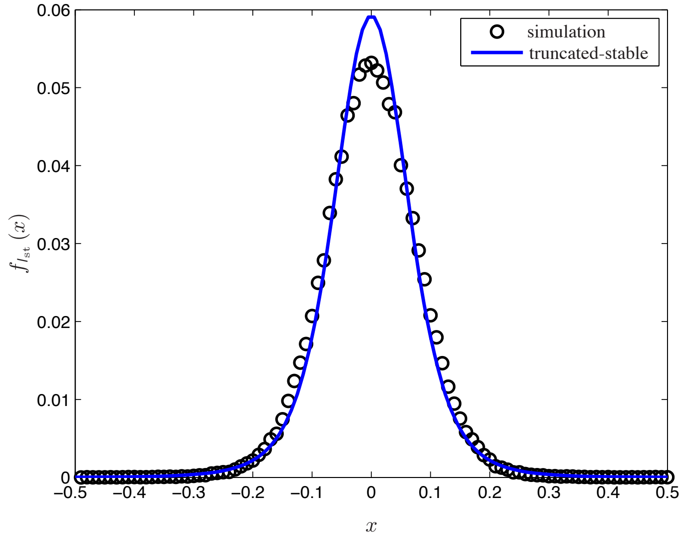

Fig. 5. PDF of the cognitive network interference I_{st} for the single-threshold protocol in the presence of shadowing with the same parameters as in Fig. 4.

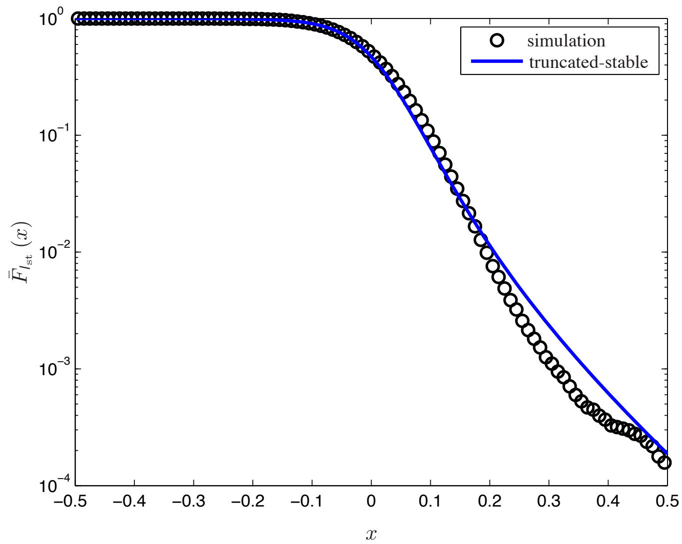

Fig. 6. CCDF of the cognitive network interference I_{st} for the single-threshold protocol in the presence of shadowing with the same parameters as in Fig. 4.

$(a_1, b_1) = (d_{\min}, d)$ and $(a_2, b_2) = (d, d_{\max})$, respectively. The nth cumulant of the cognitive network interference for the single-threshold protocol in the presence of shadowing can be written as

$$\kappa_{I_{\mathrm{st}}}(n) = \sum_{\ell=0}^{L} P_{\mathrm{I},\ell}^{n/2} \kappa_{Z_{\mathrm{st}}(\zeta\breve{\beta}_\ell;\mathcal{R}_\ell)}(n), \tag{30}$$

where the cumulant $\kappa_{Z_{\mathrm{st}}(\zeta\breve{\beta}_\ell;\mathcal{R}_\ell)}(n)$ is obtained from $\kappa_{Z_{\mathrm{st}}(\zeta;\mathcal{R})}(n)$ in (38) by replacing ζ, 2π, $d_{\min}$, and $d_{\max}$ with $\zeta\breve{\beta}_\ell$, θ_ℓ, a_ℓ, and b_ℓ, respectively. Fig. 4 shows realization snapshots of active secondary users regulated by the single-threshold protocol with $\zeta = -40$ dBm in the region prescribed by $d_{\min} = 1$ meter and $d_{\max} = 60$ meters for $\lambda = 0.01$ users$/m^2$. The shadowing is characterized by two obstacles present at 10 and 25 meters from the primary receiver, covering the angle of $\pi/2$ and causing additional attenuation of 20 dB. Accordingly, we set $\theta_1 = \theta_2 = \pi/2$, and $\breve{\beta}_1 = \breve{\beta}_2 = 20$ dB. Figs. 5 and 6 show the PDF and CCDF of the cognitive network interference I_{st} in this situation. From these figures, we can observe again that the truncated-stable model captures a remarkably accurate statistical behavior of the cognitive network interference.

IV. Applications

A. Effect of the Primary Network Power Control

Power control is often used in cellular systems to overcome the near-far problem. If the primary network uses power control, the transmitting power of the primary user varies depending on the distance R_{p} and channel gain H_{p} between the base station and primary receiver. Therefore, the transmit power P_{p} is random and it is important to understand the effect of power control on the cognitive network interference. Under perfect power control, P_{p} is set such that $P_{\mathrm{p}}|H_{\mathrm{p}}|^2/(R_{\mathrm{p}}^{2b}) \geq P^\star$, where $P^\star$ is the minimum required power level. For discrete power control, the set of possible power levels are finite. Assuming that there are L possible transmit power levels $P_1, P_2, \ldots, P_L$, we have the following probability mass function (PMF) for P_{p} at these power levels:

$$\mathbb{P}\{P_{\mathrm{p}} = P_\ell\} = \begin{cases} \mathbb{P}\left\{\frac{P^\star R_{\mathrm{p}}^{2b}}{|H_{\mathrm{p}}|^2} \leq P_1\right\}, & \text{for } \ell = 1, \\ \mathbb{P}\left\{P_{\ell-1} < \frac{P^\star R_{\mathrm{p}}^{2b}}{|H_{\mathrm{p}}|^2} \leq P_\ell\right\}, & \text{for } \ell = 2, 3, \ldots, L-1, \\ \mathbb{P}\left\{\frac{P^\star R_{\mathrm{p}}^{2b}}{|H_{\mathrm{p}}|^2} > P_L\right\}, & \text{for } \ell = L, \end{cases} \tag{31}$$

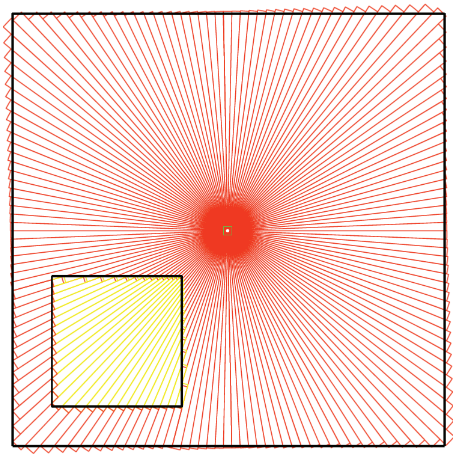

Fig. 7. Circular-section approximation of the non-circular region. The green square represents the primary user. Different colored sections correspond to different secondary user densities.

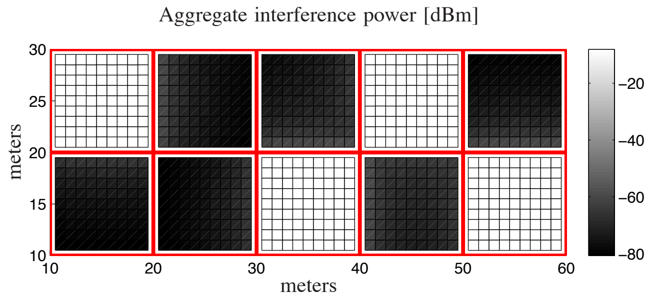

Fig. 8. Aggregate interference power (dBm) generated by FBSs placed with density $\lambda = 0.01$ FBSs$/m^2$ in the first and fourth apartments of the first row and in the third and fifth apartments of the second row for $P_{\rm I} = 0$ dBm, walls absorbing 20 dB of the radio signal, and $|H_i| \sim \mathsf{Nakagami}\,(2, 1)$.

which can be determined empirically. In this case, the nth cumulant of the cognitive network interference for the single-threshold protocol can be written as

$$\begin{aligned}\kappa_{I_{\rm st}}(n) &= \mathbb{E}\left\{P_{\rm I}^{n/2}\kappa_{Z_{\rm st}\left(\frac{\beta}{KP_{\rm p}};\mathcal{R}\right)}(n)\right\}\\ &= P_{\rm I}^{n/2}\sum_{\ell=1}^{L}\mathbb{P}\left\{P_{\rm p}=P_\ell\right\}\kappa_{Z_{\rm st}\left(\frac{\beta}{KP_\ell};\mathcal{R}\right)}(n). \end{aligned} \qquad (32)$$

B. Effect of Secondary Interference Avoidance

Instead of allowing all the active secondary users in the same class to transmit at the same power, we can also employ secondary power control, which will be effective in reducing interference and improving power efficiency [60], [61]. In addition, we can effectively design a more power-efficient secondary network if the knowledge of the secondary users' positions is available. For example, each secondary user avoids transmitting using on-off power control if the average received signal-to-noise ratio at its desired receiver is very low. Hence, with the location-awareness, we can regulate each secondary user to transmit only if its desired secondary receiver is within a certain maximum transmission range $R^\star$, which corresponds to the maximum distance beyond which reliable transmission is not possible. Let $P_{\rm s}$ and $R_{\rm s}$ be the random variables that represent the secondary transmit power and the distance from the intended receiver, respectively. Then, for the single-threshold spatial reuse protocol with power control, the nth cumulant of the cognitive network interference becomes:[9]

$$\kappa_{I_{\rm st}}(n) = \mu_{\sqrt{P_{\rm s}}}(n)\,\kappa_{Z_{\rm st}(\zeta;\mathcal{R})}(n). \qquad (33)$$

[9]The nth moment $\mu_{\sqrt{P_{\rm s}}}(n)$ depends on the power control and intended receiver selection strategies of the secondary network. For example, we have $P_{\rm s} \sim P_{\rm I}\,\mathsf{Bern}\left(F_{R_{\rm s}}(R^\star)\right)$ for the on-off secondary power control with the maximum transmission range $R^\star$. Hence,

$$\mu_{\sqrt{P_{\rm s}}}(n) = P_{\rm I}^{n/2}F_{R_{\rm s}}(R^\star),$$

and $\mu_{\sqrt{P_{\rm s}}}(n) \to P_{\rm I}^{n/2}$ as $R^\star \to \infty$ (no power control).

If the intended receiver is the nearest neighbor, then $R_{\rm s} \sim \mathsf{Rayleigh}\left(1/\left(2\pi\lambda_{\rm r}\right)\right)$ follows from the properties of Poisson point processes, where $\lambda_{\rm r}$ is the density of secondary receivers.

C. Non-circular Regions

When the primary and secondary users are confined in a limited or finite region, the position of the primary user and the shape of the region affect the distribution of the distance between the primary and secondary users and, therefore, also that of the aggregate interference. In the framework developed in Sections II and III, we implicitly consider the polar coordinate system and place the primary user at the center of the region. This coordinate system is natural for analyzing the interferers scattered in a circular section. To extend this framework to a non-circular region, we can first divide the area of interest into infinitesimal circular sections (see for example, Fig. 7) and use (30) to approximate the nth cumulant of the cognitive network interference. Using this approach, we can also consider any position of the primary user, shadowing with multiple obstacles, and areas with different densities within the region of interest.

Remark 3 (Femtocells): We can apply the approach for non-circular regions to model the aggregate interference generated by femtocell base stations (FBSs) in the macrocell networks [62]. Since the FBSs are randomly deployed without any coordination with the macrocell network, they can cause harmful interference to the macrocell users. For example, using (30) with the cumulants for the full network activity (10) instead of $\kappa_{Z_{\rm st}(\zeta\breve{\beta}_\ell;\mathcal{R}_\ell)}(n)$, we can characterize the statistics of the aggregate interference generated by the FBSs in any environment. In Fig. 8, the aggregate interference is calculated in one of the reference environments chosen in the femtocells standardization process. Each large square represents a (10×10)-meter square apartment. Each small square represents a point where the aggregate interference power is measured, which corresponds to the interference affecting a macrocell user.

D. BEP Analysis

Consider a binary phase-shift keying (BPSK) narrowband system in the presence of interference generated by the cognitive network confined within the region $\mathcal{R}$, where transmission

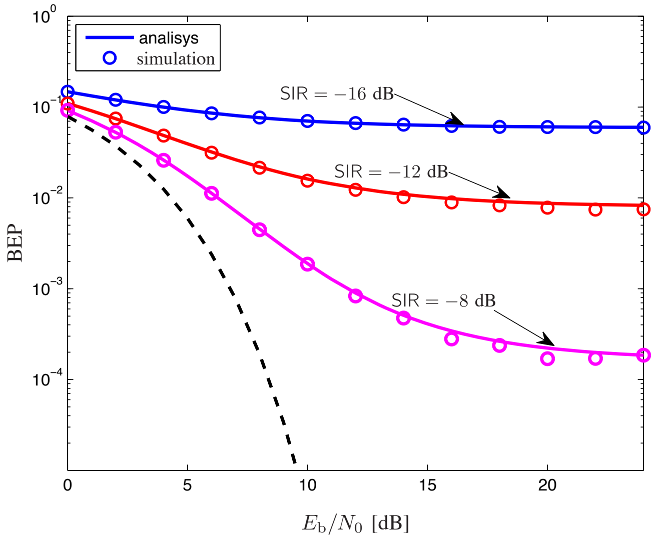

Fig. 9. BEP of BPSK versus $E_{\rm b}/N_0$ in the presence of the cognitive network interference $I_{\rm st}$ for the single-threshold protocol when SIR $= -16$, -12, and -8 dB. $\lambda = 0.1$ users$/m^2$ and $\zeta = -40$ dBm. For comparison, the BEP in the absence of interference is also plotted (dashed line).

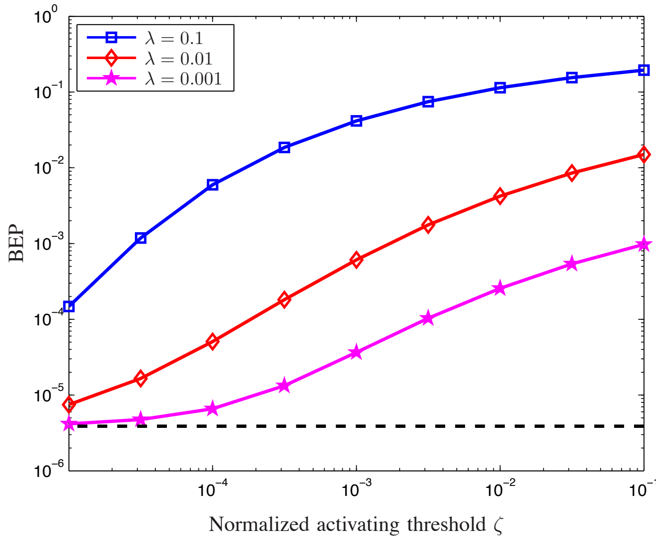

Fig. 10. BEP of BPSK as a function of the normalized activating threshold ζ for the single-threshold protocol when $\lambda = 0.1$, 0.01, and 0.001 users$/m^2$. $E_{\rm b}/N_0 = 10$ dB and SIR $= -10$ dB. For comparison, the BEP in the absence of interference is also plotted (dashed line).

activities of the nodes are regulated according to (3). The decision variable of the primary received symbol after the correlation receiver can be written as

$$V = GU\sqrt{E_{\rm b}} + I_{\rm st} + W\,, \tag{34}$$

where G is the channel fading affecting the victim signal; $U \in \{1, -1\}$ is the information data; $E_{\rm b}$ is the energy per bit; $I_{\rm st}$ is the congnitive network interference; and W is the zero-mean additive white Gaussian noise with variance $N_0/2$. Conditioned on G, $I_{\rm st}$, and $U = +1$, the CF of the decision variable V can be written as

$$\begin{aligned} &\psi_V\left(j\omega \middle| G, I_{\rm st}, U = +1\right) \\ &\quad = \exp\left\{ j\omega\left(G\sqrt{E_{\rm b}} + I_{\rm st}\right) - \frac{N_0\omega^2}{4}\right\}. \end{aligned} \tag{35}$$

Assuming that G and $I_{\rm st}$ are statistically independent, the CF of the decision variable conditioned on $U = +1$ is given by

$$\psi_V\left(j\omega \middle| U = +1\right) = \psi_G\left(j\omega\sqrt{E_{\rm b}}\right)\psi_{I_{\rm st}}(j\omega)\exp\left(-\frac{N_0\omega^2}{4}\right). \tag{36}$$

For the cognitive network interference $I_{\rm st}$, we use the symmetric truncated-stable model $I_{\rm st} \sim \mathcal{S}_{\rm t}\left(\gamma'_{\rm st}, \alpha = 2/b, g_{\rm st}\right)$, where the parameters $\gamma'_{\rm st}$ and $g_{\rm st}$ are determined by using (25) and (26), respectively. Since $I_{\rm st}$ is approximated as a symmetric random variable, the average BEP is equal to the BEP conditioned on $U = +1$, which can be expressed, using the inversion theorem [63], as

$$\begin{aligned} P_{\rm e} &= \mathbb{P}\left\{V < 0 \middle| U = +1\right\} \\ &= \frac{1}{2} + \frac{1}{2\pi}\int_0^{\infty} \frac{\psi_V\left(-j\omega \middle| U = +1\right) - \psi_V\left(+j\omega \middle| U = +1\right)}{j\omega}\, d\omega. \end{aligned} \tag{37}$$

V. Numerical Results

In this section, we illustrate the use of cognitive network interference model to provide insight into the coexistence between primary and secondary networks. In numerical examples, we consider $d_{\min} = 1$ meter, $d_{\max} = 60$ meters, b = 1.5, and Rayleigh fading for both primary and secondary signals unless differently specified. We first investigate the effect of the cognitive network interference on the BEP performance of the primary user. In Fig. 9, the BEP of BPSK versus $E_{\rm b}/N_0$ is depicted at the signal-to-interference ratio SIR $\triangleq E_{\rm b}/P_{\rm I} = -16$, -12, and -8 dB when the secondary network having density $\lambda = 0.1$ users$/m^2$ employs the single-threshold protocol with $\zeta = -40$ dBm. We can observe from Fig. 9 that the simulation agrees well with the analytical results, which confirms the BEP analysis in Section IV-D and again validates the truncated-stable interference model.

To ascertain the effect of the activating threshold and spatial density of secondary users on the primary BEP performance, Fig. 10 shows the BEP of BPSK as a function of the normalized activity threshold ζ for the single-threshold protocol at $E_{\rm b}/N_0 = 10$ dB and SIR $= -10$ dB when $\lambda = 0.1$, 0.01, and 0.001 users$/m^2$. As expected, we can observe that the primary BEP degrades severely as the node density λ and/or the threshold ζ increase. For a given secondary density, our analytical framework enables us to design an activity threshold that guarantees a target BEP at the primary user.

To demonstrate the effect of fading on the cognitive network interference, we next consider Nakagami-m fading for both primary and secondary signals, i.e., $\sqrt{Y_i} \sim$ Nakagami$(m, 1)$ and $|H_i| \sim$ Nakagami$(m, 1)$. Fig. 11 shows the variance (or equivalently, average power) of the cognitive network interference $I_{\rm st}$ as a function of the maximum distance $d_{\max}$ from the primary user for Nakagami fading parameters $m = 1$, 3, and 5. The secondary network has the user density $\lambda = 0.01$ users$/m^2$, each transmits with $P_{\rm I} = 0$ dBm according to the single-threshold protocol with $\zeta = -30$ dBm. This

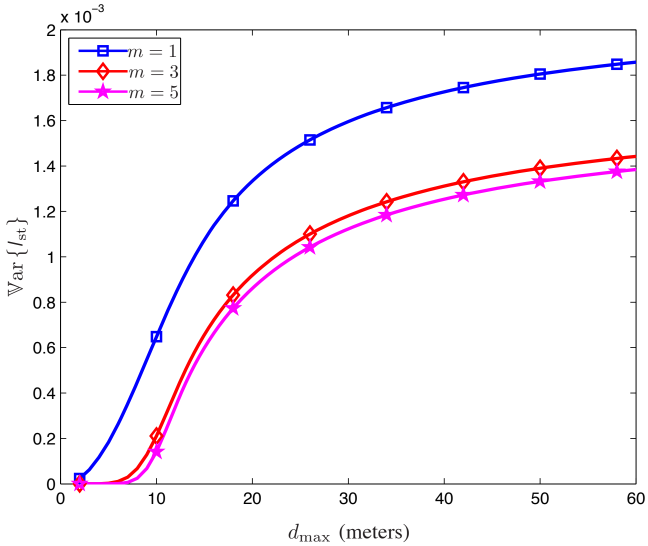

Fig. 11. Variance of the cognitive network interference $I_{\rm st}$ for the single-threshold protocol as a function of the maximum distance $d_{\max}$ of the region $\mathcal{R}$ when the Nakagami fading parameters $m = 1$, 3, and 5. $\lambda = 0.01$ users$/m^2$, $\zeta = -30$ dBm, $P_{\rm I} = 0$ dBm, and Nakagami-m fading for primary and secondary links $\sqrt{Y_i} \sim \mathsf{Nakagami}\,(m, 1)$ and $|H_i| \sim \mathsf{Nakagami}\,(m, 1)$.

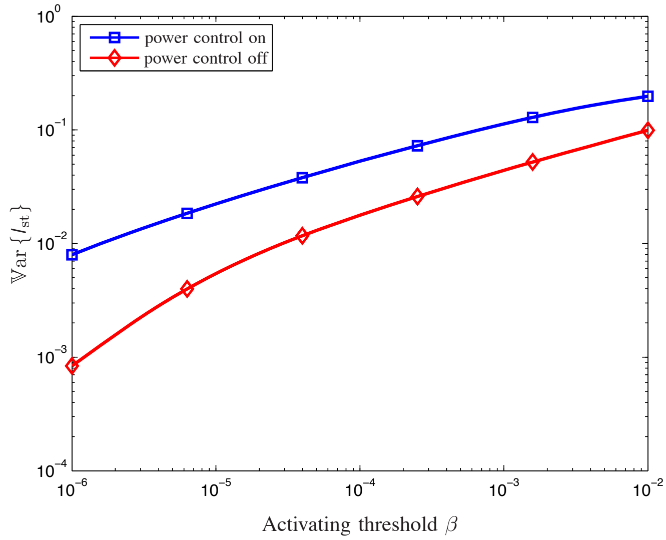

Fig. 12. Variance of the cognitive network interference $I_{\rm st}$ for the single-threshold protocol in the presence of primary power control as a function of the activating threshold β. $\lambda = 0.1$ users$/m^2$, $K = 0$ dBm, $P_{\rm I} = 0$ dBm, $|H_{\rm p}| \sim \mathsf{Rayleigh}\,(1/2)$, $d_{\min_{\rm p}} = 1$ meter, and $d_{\max_{\rm p}} = 1000$ meters. The power levels of the primary user are -5, -15, -25, and -35 dBm with the minimum required power level $P^\star = -95$ dBm.

example reveals that for a fixed threshold ζ, as the fading parameter m increases (less severe fading), the cognitive network interference vanishes at the primary user due to rare secondary activity. We can also see that milder fading (i.e., larger m) reduces the cognitive network interference power for all the values of $d_{\max}$. This is due to the fact that milder fading decreases the activity of the secondary users in the proximity of the primary user, leading consequently to a lower cognitive interference power. Moreover, we observe that the cognitive network interference power tends to saturate as $d_{\max}$ increases since secondary users located far from the primary user contribute marginally to aggregate interference.

The effect of power control on the cognitive network interference is illustrated in Fig. 12, where the variance of the cognitive network interference $I_{\rm st}$ for the single-threshold protocol as a function of the activating threshold β is depicted in the presence of primary power control. In this example, $K = 0$ dBm and the density and transmit power of the secondary users are $\lambda = 0.1$ users$/m^2$ and $P_{\rm I} = 0$ dBm, respectively. The primary user is distributed in a circular area defined by minimum and maximum distances $d_{\min_{\rm p}} = 1$ meter and $d_{\max_{\rm p}} = 1000$ meters from the base station, respectively, and its communication link experiences Rayleigh fading, i.e., $|H_{\rm p}| \sim \mathsf{Rayleigh}\,(1/2)$. For the primary power control policy, we set four power levels -5, -15, -25, -35 in dBm and the minimum required power level to $P^\star = -95$ dBm. We can see from the figure that if the primary network uses power control, the variance of the cognitive network interference increases for all the values of β. This is due to the fact that when the primary user is close to the base station, its transmission power decreases. As a consequence, the secondary users will increase their activity, leading to a larger number of active secondary users.

In Fig. 13, the variance of the cognitive network interference $I_{\rm fa}$ as a function of the maximum transmission range $R^\star$ of the secondary users for the case of full activity (i.e., $\zeta \to \infty$) is depicted in the presence of the on-off secondary power control for various values of λ. In this example, $\sqrt{Y_i} \sim \mathsf{Nakagami}\,(2, 1)$ and $|H_i| \sim \mathsf{Nakagami}\,(2, 1)$. For the secondary power control policy, we set $P_{\rm I} = 0$ dBm, $P_{\rm s} \sim \mathsf{Bern}\,(F_{R_{\rm s}}(R^\star))$, $R_{\rm s} \sim \mathsf{Rayleigh}\,(1/(2\pi\lambda_{\rm r}))$, and $\lambda_{\rm r} = \lambda$. Hence, $\mu_{\sqrt{P_{\rm s}}}(n)$ in (33) becomes $1 - e^{-\pi\lambda_{\rm r}R^{\star 2}}$, which reveals that the interference power increases and approaches exponentially to one (i.e., $P_{\rm I} = 0$ dBm without power control) as the transmission range $R^\star$ increases. We can see from Fig. 13 that the cognitive interference power reduces, especially at low values of λ, as the range $R^\star$ decreases.

Fig. 14 shows the PDFs of the cognitive network interference $I_{\rm fa}$ at the primary user in a (200×200)-meter square (see Fig. 7) for the case of full activity ($\zeta \to \infty$) and $P_{\rm I} = 0$ dBm. The primary and secondary links have Nakagami-m fading, i.e., $\sqrt{Y} \sim \mathsf{Nakagami}\,(2, 1)$ and $|H_i| \sim \mathsf{Nakagami}\,(2, 1)$; and the square region has two different secondary spatial densities: $\lambda = 0.01$ in the red sections and $\lambda = 0$ (i.e., no secondary users) in the yellow sections. The PDFs $f_{I_{\rm fa}}(x)$ are plotted for three cases of the primary user location: i) at the center of the large square, ii) at the center of the low (zero) density region, and iii) at the top-right corner of the large square. We can observe from Fig. 14 that the cognitive network interference becomes less severe as the primary user moves to the corner. This is due to the fact that the distance between the primary and secondary users increases when the primary user is located at the corner. Moreover, using this framework, we can also consider a nonuniform spatial distribution of the secondary users in the region of interest. Therefore, our statistical interference model enables us to characterize the position where the primary user is less vulnerable to the effect of cognitive network interference.

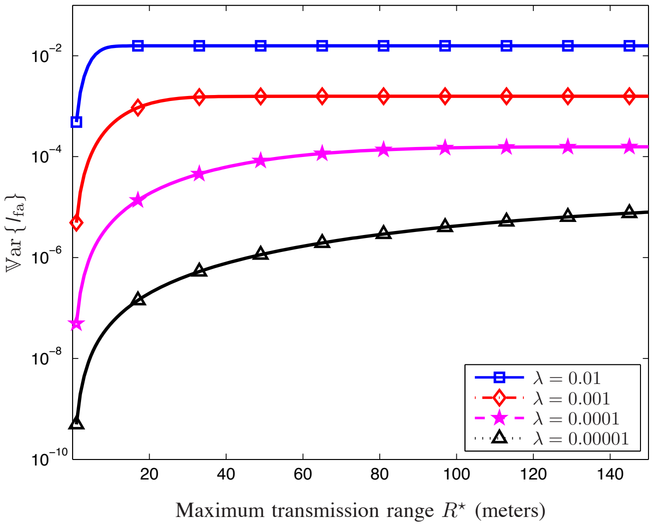

Fig. 13. Variance of the cognitive network interference I_{fa} for full activity ($\zeta \to \infty$) in the presence of the on-off secondary power control as a function of the maximum transmission range $R^\star$ of the secondary users when $\lambda = 0.01$, 0.001, 0.0001, and 0.00001 users$/m^2$. $P_{\mathrm{I}} = 0$ dBm, $P_{\mathrm{s}} \sim \mathsf{Bern}\left(F_{R_{\mathrm{s}}}(R^\star)\right)$, $R_{\mathrm{s}} \sim \mathsf{Rayleigh}\left(1/(2\pi\lambda_{\mathrm{r}})\right)$, $\lambda_{\mathrm{r}} = \lambda$, and Nakagami-$m$ fading for primary and secondary links $\sqrt{Y_i} \sim \mathsf{Nakagami}(2,1)$ and $|H_i| \sim \mathsf{Nakagami}(2,1)$.

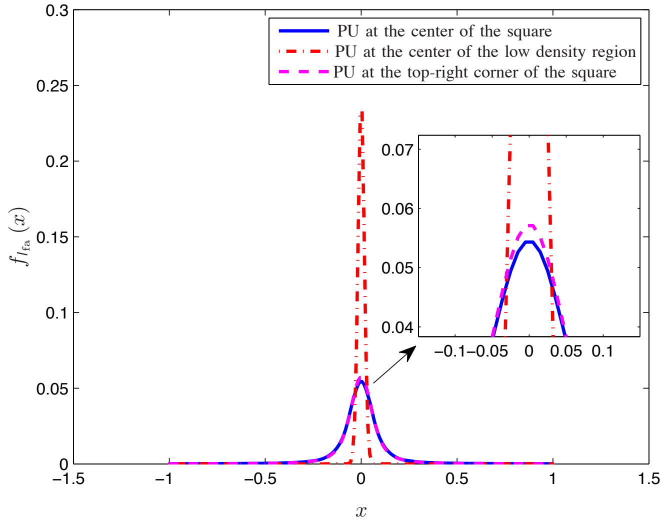

Fig. 14. PDF of the cognitive network interference I_{fa} at the primary user (PU) in a (200×200)-meter square (see Fig. 7) for full activity ($\zeta \to \infty$). $P_{\mathrm{I}} = 0$ dBm and Nakagami-m fading for primary and secondary links $\sqrt{Y_i} \sim \mathsf{Nakagami}(2,1)$ and $|H_i| \sim \mathsf{Nakagami}(2,1)$. The secondary spatial density is equal to $\lambda = 0.01$ users$/m^2$ in the red sections, whereas $\lambda = 0$ users$/m^2$ (i.e., no secondary users) in the yellow sections.

VI. Conclusions

In this paper, we proposed a new statistical model for aggregate interference of cognitive networks, which accounts for the sensing procedure, the spatial distribution of nodes, secondary spatial reuse protocol, and environment-dependent conditions such as path loss, shadowing, and channel fading. We considered two types of secondary spatial reuse protocols, namely, single-threshold and multiple-threshold protocols. For each protocol, we derived the characteristic function and the cumulant of the cognitive network interference at the primary user. By using the truncated-stable distributions, we obtained the statistical model for the cognitive network interference. We further extended this model to include the effect of power control and shadowing, and derived the BEP in the presence of cognitive network interference. Numerical results demonstrated the effectiveness of our model for capturing the statistical behavior of the cognitive network interference in a variety of scenarios. The framework developed in the paper enables us to characterize cognitive network interference for successful deployment of future cognitive networks. Furthermore, this framework can also be applied in the study of the effect of inter-tier interference caused by randomly deployed closed-access femtocells on the macrocell users in multi-tier networks.

Appendix A
Glossary of Statistical Symbols

We adopt the convention of using upper-case letters without serifs for random variables and the corresponding lower-case letters with serifs for their realizations and dummy arguments.

$\mathbb{E}\{\cdot\}$	Expectation operator
$\mathbb{P}\{\cdot\}$	Probability measure
$f_X(x)$	Probability density function of X
$F_X(x)$	Cumulative distribution function of X
$\bar{F}_X(x)$	Complementary cumulative distribution function of X: $\bar{F}_X(x) = 1 - F_X(x)$
$\psi_X(j\omega)$	Characteristic function of X: $\psi_X(j\omega) \triangleq \mathbb{E}\left\{e^{j\omega X}\right\}$ where $j = \sqrt{-1}$
$\mu_X(n)$	nth moment of X: $\mu_X(n) \triangleq \mathbb{E}\{X^n\}$
$\mu_X^{(\mathrm{pt})}(n,l,u)$	nth partial moment of X calculated within the interval $[l,u]$: $\mu_X^{(\mathrm{pt})}(n,l,u) \triangleq \int_l^u x^n f_X(x)\,dx$
$\kappa_X(n)$	nth cumulant of X: $\kappa_X(n) \triangleq \frac{1}{j^n} \frac{d^n \ln \psi_X(j\omega)}{d\omega^n}\Big\vert_{\omega=0}$
$\mathsf{Bern}(p)$	Bernoulli distribution with mean p: if $X \sim \mathsf{Bern}(p)$, then $\mathbb{P}\{X=1\} = p$ and $\mathbb{P}\{X=0\} = 1-p$
$\mathcal{S}_{\mathrm{t}}(\gamma', \alpha, g)$	Symmetric truncated-stable distribution with the dispersion γ', characteristic exponent α, and smoothing parameter g
$\mathsf{Rayleigh}(\sigma^2)$	Rayleigh distribution with the parameter σ^2: $f_X(x) = \frac{x}{\sigma^2}\exp\left(-\frac{x^2}{2\sigma^2}\right),\ x \geq 0$
$\mathsf{Nakagami}(m,\Omega)$	Nakagami distribution with the fading severity parameter m and power parameter Ω: $f_X(x) = \frac{2m^m x^{2m-1}}{\Omega^m \Gamma(m)}\exp\left(-\frac{mx^2}{\Omega}\right)$, $x \geq 0$

APPENDIX B
DERIVATIONS OF THE CUMULANTS

A. Cumulant of $Z_{\mathrm{st}}(\zeta;\mathcal{R})$ for the Single-Threshold Protocol

We start by deriving the nth cumulant of $Z_{\mathrm{st}}(\zeta;\mathcal{R})$ in (12) for the single-threshold protocol. Using (14), we obtain

$$\begin{aligned}
\kappa_{Z_{\mathrm{st}}(\zeta;\mathcal{R})}(n) &= 2\pi\lambda \int_X \int_Y \int_{d_{\min}}^{d_{\max}} x^n r^{1-nb} \mathbb{1}_{[0,\zeta]}\left(r^{-2b}y\right) \\
&\qquad \times f_X(x)\, f_Y(y)\, dr dy dx \\
&= 2\pi\lambda\, \mu_X(n) \int_0^{d_{\max}^{2b}\zeta} \int_{\max\left\{d_{\min},(y/\zeta)^{\frac{1}{2b}}\right\}}^{d_{\max}} r^{1-nb} f_Y(y)\, dr dy \\
&= 2\pi\lambda\, \mu_X(n) \int_0^{d_{\min}^{2b}\zeta} \int_{d_{\min}}^{d_{\max}} r^{1-nb} f_Y(y)\, dr dy \\
&\quad + 2\pi\lambda\, \mu_X(n) \int_{d_{\min}^{2b}\zeta}^{d_{\max}^{2b}\zeta} \int_{(y/\zeta)^{\frac{1}{2b}}}^{d_{\max}} r^{1-nb} f_Y(y)\, dr dy \\
&= \frac{2\pi\lambda\, \mu_X(n)}{nb-2} \int_0^{d_{\min}^{2b}\zeta} \left(d_{\min}^{2-nb} - d_{\max}^{2-nb}\right) f_Y(y)\, dy \\
&\quad + \frac{2\pi\lambda\, \mu_X(n)}{nb-2} \int_{d_{\min}^{2b}\zeta}^{d_{\max}^{2b}\zeta} \left[(y/\zeta)^{\frac{2-nb}{2b}} - d_{\max}^{2-nb}\right] f_Y(y)\, dy \\
&= \frac{2\pi\lambda\, \mu_X(n)}{nb-2} \Bigg[\left(d_{\min}^{2-nb} - d_{\max}^{2-nb}\right) F_Y\left(d_{\min}^{2b}\zeta\right) \\
&\qquad + \zeta^{\frac{nb-2}{2b}} \mu_Y^{(\mathrm{pt})}\left(\frac{2-nb}{2b}, d_{\min}^{2b}\zeta, d_{\max}^{2b}\zeta\right) \\
&\qquad - d_{\max}^{2-nb} \mu_Y^{(\mathrm{pt})}\left(0, d_{\min}^{2b}\zeta, d_{\max}^{2b}\zeta\right)\Bigg].
\end{aligned} \tag{38}$$

B. Cumulants of $Z_k(\mathcal{R})$ ($k = 1, 2, \ldots, N$) for the Multiple-Threshold Protocol

We now derive the nth cumulant of $Z_k(\mathcal{R})$ in (17) for $\mathcal{A}_k$ of the multiple-threshold protocol. Using (19), we obtain

$$\begin{aligned}
\kappa_{Z_k(\mathcal{R})}(n) &= 2\pi\lambda \int_X \int_Y \int_{d_{\min}}^{d_{\max}} x^n r^{1-nb} \mathbb{1}_{[\zeta_{k-1},\zeta_k]}\left(r^{-2b}y\right) \\
&\qquad \times f_X(x)\, f_Y(y)\, dr dy dx \\
&= 2\pi\lambda\, \mu_X(n) \int_{d_{\min}^{2b}\zeta_{k-1}}^{d_{\max}^{2b}\zeta_k} \int_{\max\left\{d_{\min},(y/\zeta_k)^{\frac{1}{2b}}\right\}}^{\min\left\{d_{\max},(y/\zeta_{k-1})^{\frac{1}{2b}}\right\}} r^{1-nb} \\
&\qquad \times f_Y(y)\, dr dy.
\end{aligned} \tag{39}$$

1) $k = 1$: It is obvious from (39) that

$$\kappa_{Z_1(\mathcal{R})}(n) = \kappa_{Z_{\mathrm{st}}(\zeta_1;\mathcal{R})}(n). \tag{40}$$

2) $k = 2, 3, \ldots, N-1$: We can evaluate the integral in (39) by dividing the integration interval of y into three disjoint ones, namely:

$$\begin{aligned}
d_{\min}^{2b}\zeta_{k-1} &\le y < \min\left\{d_{\max}^{2b}\zeta_{k-1}, d_{\min}^{2b}\zeta_k\right\}, \\
\min\left\{d_{\max}^{2b}\zeta_{k-1}, d_{\min}^{2b}\zeta_k\right\} &\le y < \max\left\{d_{\max}^{2b}\zeta_{k-1}, d_{\min}^{2b}\zeta_k\right\}, \\
\max\left\{d_{\max}^{2b}\zeta_{k-1}, d_{\min}^{2b}\zeta_k\right\} &\le y \le d_{\max}^{2b}\zeta_k,
\end{aligned}$$

involving two different cases $d_{\min}^{2b}\zeta_k \ge d_{\max}^{2b}\zeta_{k-1}$ and $d_{\min}^{2b}\zeta_k < d_{\max}^{2b}\zeta_{k-1}$.

i) *Case $d_{\min}^{2b}\zeta_k \ge d_{\max}^{2b}\zeta_{k-1}$:* In this case, we have

$$\begin{aligned}
&\kappa_{Z_k(\mathcal{R})}(n) \\
&= \Bigg[2\pi\lambda\, \mu_X(n) \int_{d_{\min}^{2b}\zeta_{k-1}}^{d_{\max}^{2b}\zeta_{k-1}} \int_{d_{\min}}^{(y/\zeta_{k-1})^{\frac{1}{2b}}} r^{1-nb} f_Y(y)\, dr dy \\
&\quad + \int_{d_{\max}^{2b}\zeta_{k-1}}^{d_{\min}^{2b}\zeta_k} \int_{d_{\min}}^{d_{\max}} r^{1-nb} f_Y(y)\, dr dy \\
&\quad + \int_{d_{\min}^{2b}\zeta_k}^{d_{\max}^{2b}\zeta_k} \int_{(y/\zeta_k)^{\frac{1}{2b}}}^{d_{\max}} r^{1-nb} f_Y(y)\, dr dy\Bigg]
\end{aligned} \tag{41}$$

$$\begin{aligned}
&= \frac{2\pi\lambda\, \mu_X(n)}{nb-2} \Bigg[d_{\min}^{2-nb} \mu_Y^{(\mathrm{pt})}\left(0, d_{\min}^{2b}\zeta_{k-1}, d_{\max}^{2b}\zeta_{k-1}\right) \\
&\quad - \zeta_{k-1}^{\frac{nb-2}{2b}} \mu_Y^{(\mathrm{pt})}\left(\frac{2-nb}{2b}, d_{\min}^{2b}\zeta_{k-1}, d_{\max}^{2b}\zeta_{k-1}\right) \\
&\quad + \left(d_{\min}^{2-nb} - d_{\max}^{2-nb}\right) \mu_Y^{(\mathrm{pt})}\left(0, d_{\max}^{2b}\zeta_{k-1}, d_{\min}^{2b}\zeta_k\right) \\
&\quad + \zeta_k^{\frac{nb-2}{2b}} \mu_Y^{(\mathrm{pt})}\left(\frac{2-nb}{2b}, d_{\min}^{2b}\zeta_k, d_{\max}^{2b}\zeta_k\right) \\
&\quad - d_{\max}^{2-nb} \mu_Y^{(\mathrm{pt})}\left(0, d_{\min}^{2b}\zeta_k, d_{\max}^{2b}\zeta_k\right)\Bigg].
\end{aligned} \tag{42}$$

ii) *Case $d_{\min}^{2b}\zeta_k < d_{\max}^{2b}\zeta_{k-1}$:* Similarly, we have

$$\begin{aligned}
&\kappa_{Z_k(\mathcal{R})}(n) \\
&= 2\pi\lambda\, \mu_X(n) \Bigg[\int_{d_{\min}^{2b}\zeta_{k-1}}^{d_{\min}^{2b}\zeta_k} \int_{d_{\min}}^{(y/\zeta_{k-1})^{\frac{1}{2b}}} r^{1-nb} f_Y(y)\, dr dy \\
&\quad + \int_{d_{\min}^{2b}\zeta_k}^{d_{\max}^{2b}\zeta_{k-1}} \int_{(y/\zeta_k)^{\frac{1}{2b}}}^{(y/\zeta_{k-1})^{\frac{1}{2b}}} r^{1-nb} f_Y(y)\, dr dy \\
&\quad + \int_{d_{\max}^{2b}\zeta_{k-1}}^{d_{\max}^{2b}\zeta_k} \int_{(y/\zeta_k)^{\frac{1}{2b}}}^{d_{\max}} r^{1-nb} f_Y(y)\, dr dy\Bigg] \\
&= \frac{2\pi\lambda\, \mu_X(n)}{nb-2} \Bigg[d_{\min}^{2-nb} \mu_Y^{(\mathrm{pt})}\left(0, d_{\min}^{2b}\zeta_{k-1}, d_{\min}^{2b}\zeta_k\right) \\
&\quad - \zeta_{k-1}^{\frac{nb-2}{2b}} \mu_Y^{(\mathrm{pt})}\left(\frac{2-nb}{2b}, d_{\min}^{2b}\zeta_{k-1}, d_{\min}^{2b}\zeta_k\right) \\
&\quad + \left(\zeta_k^{\frac{nb-2}{2b}} - \zeta_{k-1}^{\frac{nb-2}{2b}}\right) \\
&\qquad \times \mu_Y^{(\mathrm{pt})}\left(\frac{2-nb}{2b}, d_{\min}^{2b}\zeta_k, d_{\max}^{2b}\zeta_{k-1}\right) \\
&\quad + \zeta_k^{\frac{nb-2}{2b}} \mu_Y^{(\mathrm{pt})}\left(\frac{2-nb}{2b}, d_{\max}^{2b}\zeta_{k-1}, d_{\max}^{2b}\zeta_k\right) \\
&\quad - d_{\max}^{2-nb} \mu_Y^{(\mathrm{pt})}\left(0, d_{\max}^{2b}\zeta_{k-1}, d_{\max}^{2b}\zeta_k\right)\Bigg].
\end{aligned} \tag{43}$$

Now, combining (42) and (43), we obtain the nth cumulant of $Z_k(\mathcal{R})$ for $k = 2, 3, \ldots, N-1$ as follows:

$$\begin{aligned}\kappa_{Z_k(\mathcal{R})}(n) = \frac{2\pi\lambda\,\mu_X(n)}{nb-2}\Bigg[& d_{\min}^{2-nb}\mu_Y^{(\mathrm{pt})}\left(0, d_{\min}^{2b}\zeta_{k-1}, \Delta_{\min}\right) \\ & - \zeta_{k-1}^{\frac{nb-2}{2b}}\,\mu_Y^{(\mathrm{pt})}\left(\frac{2-nb}{2b}, d_{\min}^{2b}\zeta_{k-1}, \Delta_{\min}\right) \\ & + c_1\,\mu_Y^{(\mathrm{pt})}\left(c_2, \Delta_{\min}, \Delta_{\max}\right) \\ & + \zeta_k^{\frac{nb-2}{2b}}\,\mu_Y^{(\mathrm{pt})}\left(\frac{2-nb}{2b}, \Delta_{\max}, d_{\max}^{2b}\zeta_k\right) \\ & - d_{\max}^{2-nb}\mu_Y^{(\mathrm{pt})}\left(0, \Delta_{\max}, d_{\max}^{2b}\zeta_k\right)\Bigg], \end{aligned} \quad (44)$$

where $\Delta_{\min} = \min\left\{d_{\max}^{2b}\zeta_{k-1}, d_{\min}^{2b}\zeta_k\right\}$, $\Delta_{\max} = \max\left\{d_{\max}^{2b}\zeta_{k-1}, d_{\min}^{2b}\zeta_k\right\}$, and

$$\begin{aligned}&(c_1, c_2) \\ &= \begin{cases}\left(d_{\min}^{2-nb} - d_{\max}^{2-nb}, 0\right), & \text{if } d_{\min}^{2b}\zeta_k \geq d_{\max}^{2b}\zeta_{k-1} \\ \left(\zeta_k^{\frac{nb-2}{2b}} - \zeta_{k-1}^{\frac{nb-2}{2b}}, \frac{2-nb}{2b}\right), & \text{if } d_{\min}^{2b}\zeta_k < d_{\max}^{2b}\zeta_{k-1}.\end{cases}\end{aligned} \quad (45)$$

3) $k = N$: Since $\zeta_N = \infty$, it is obvious that $d_{\min}^{2b}\zeta_k \geq d_{\max}^{2b}\zeta_{k-1}$ and the third term in (41) vanishes for $k = N$. Hence, it follows immediately from (42) along with $\mu_Y^{(\mathrm{pt})}(0, a, \infty) = \bar{F}_Y(a)$ that

$$\begin{aligned}\kappa_{Z_N(\mathcal{R})}(n) = \frac{2\pi\lambda\,\mu_X(n)}{nb-2}\Bigg[& d_{\min}^{2-nb}\mu_Y^{(\mathrm{pt})}\left(0, d_{\min}^{2b}\zeta_{k-1}, d_{\max}^{2b}\zeta_{k-1}\right) \\ & - \zeta_{k-1}^{\frac{nb-2}{2b}}\,\mu_Y^{(\mathrm{pt})}\left(\frac{2-nb}{2b}, d_{\min}^{2b}\zeta_{k-1}, d_{\max}^{2b}\zeta_{k-1}\right) \\ & + \left(d_{\min}^{2-nb} - d_{\max}^{2-nb}\right)\bar{F}_Y\left(d_{\max}^{2b}\zeta_{k-1}\right)\Bigg]. \end{aligned} \quad (46)$$

REFERENCES

[1] FCC, "Policy task force report (et docket-135)," 2002.

[2] M. A. McHenry, "NSF Spectrum Occupancy Measurements Project Summary," *Shared Spectrum Company*, 2005.

[3] FCC, "Notice of proposed rule making, in the matter of facilitating opportunities for flexible, efficient and reliable spectrum use employing cognitive radio technologies (et docket no. 03-108) and authorization and use of software defined radios (et docket no. 00-47), FCC 03-322," Dec. 2003.

[4] S. Haykin, "Cognitive radio: Brain-empowered wireless communications," *IEEE J. Sel. Areas Commun.*, vol. 23, no. 2, pp. 201–220, Feb. 2005.

[5] I. F. Akyildiz, W. Lee, M. C. Vuran, and S. Mohanty, "Next generation/dynamic spectrum access/cognitive radio wireless networks: A survey," *Computer Networks*, vol. 50, no. 13, pp. 2127–2159, Sep. 2006.

[6] Q. Zhao and B. M. Sadler, "A survey of dynamic spectrum access," *IEEE Signal Process. Mag.*, vol. 24, no. 3, pp. 79–89, May 2007.

[7] A. Goldsmith, S. A. Jafar, I. Maric, and S. Srinivasa, "Breaking spectrum gridlock with cognitive radios: An information theoretic perspective," *Proc. IEEE*, vol. 97, no. 5, pp. 894–914, May 2009.

[8] A. Ghasemi, , and E. S. Sousa, "Spectrum sensing in cognitive radio networks: Requirements, challenges and design trade-offs," *IEEE Commun. Mag.*, vol. 46, no. 4, pp. 32–39, Apr. 2008.

[9] D. Cabric, S. M. Mishra, and R. W. Brodersen, "Implementation issues in spectrum sensing for cognitive radios," in *Proc. IEEE Asilomar Conf. on Signals, Systems, and Computers*, Pacific Grove, CA, Nov. 2004, pp. 772–776.

[10] A. Sonnenschein and P. M. Fishman, "Radiometric detection of spread-spectrum signals in noise," *IEEE Trans. Aerosp. Electron. Syst.*, vol. 28, no. 3, pp. 654–660, Jul. 1992.

[11] R. Tandra and A. Sahai, "SNR walls for signal detection," *IEEE J. Sel. Topics Signal Process.*, vol. 2, no. 1, pp. 4–17, Feb. 2008.

[12] R. Tandra, S. M. Mishra, and A. Sahai, "What is a spectrum hole and what does it take to recognize one: Extended version," *Proc. IEEE*, vol. 97, no. 5, pp. 824–848, May 2009.

[13] M. Z. Win, "A mathematical model for network interference," *IEEE Commun. Theory Workshop*, Sedona, AZ, May 2007.

[14] M. Z. Win, P. C. Pinto, and L. A. Shepp, "A mathematical theory of network interference and its applications," *Proc. IEEE*, vol. 97, no. 2, pp. 205–230, Feb. 2009.

[15] M. Z. Win and R. A. Scholtz, "Impulse radio: How it works," *IEEE Commun. Lett.*, vol. 2, no. 2, pp. 36–38, Feb. 1998.

[16] ——, "Ultra-wide bandwidth time-hopping spread-spectrum impulse radio for wireless multiple-access communications," *IEEE Trans. Commun.*, vol. 48, no. 4, pp. 679–691, Apr. 2000.

[17] M. Z. Win, "A unified spectral analysis of generalized time-hopping spread-spectrum signals in the presence of timing jitter," *IEEE J. Sel. Areas Commun.*, vol. 20, no. 9, pp. 1664–1676, Dec. 2002.

[18] R. A. Scholtz, "Private conversation," University of Southern California, Sep. 1997, Los Angeles, CA.

[19] J. H. Winters, "Private conversation," AT&T Labs-Research, Mar. 2001, Middletown, NJ.

[20] L. A. Shepp, "Private conversation," AT&T Labs-Research, Mar. 2001, Middletown, NJ.

[21] P. C. Pinto and M. Z. Win, "Communication in a Poisson field of interferers – Part I: Interference distribution and error probability," *IEEE Trans. Wireless Commun.*, vol. 9, no. 7, pp. 2176–2186, Jul. 2010.

[22] ——, "Communication in a Poisson field of interferers – Part II: Channel capacity and interference spectrum," *IEEE Trans. Wireless Commun.*, vol. 9, no. 7, pp. 2187–2195, Jul. 2010.

[23] A. Rabbachin, T. Q. S. Quek, P. C. Pinto, I. Oppermann, and M. Z. Win, "Non-coherent UWB communication in the presence of multiple narrowband interferers," *IEEE Trans. Wireless Commun.*, vol. 9, no. 11, pp. 3365-3379, Nov. 2010.

[24] P. C. Pinto, A. Giorgetti, M. Z. Win, and M. Chiani, "A stochastic geometry approach to coexistence in heterogeneous wireless networks," *IEEE J. Sel. Areas Commun.*, vol. 27, no. 7, pp. 1268–1282, Sep. 2009.

[25] P. C. Pinto and M. Z. Win, "Spectral characterization of wireless networks," *IEEE Wireless Commun. Mag.*, vol. 14, no. 6, pp. 27–31, Dec. 2007.

[26] J. F. Kingman, *Poisson Processes*. Oxford University Press, 1993.

[27] S. Chandrasekhar, "Stochastic problems in physics and astronomy," *Rev. Modern Phys.*, vol. 15, no. 1, pp. 1–89, Jan. 1943.

[28] S. E. Heath, "*Applications of the Poisson Model to Wireless Telephony and to Cosmology*," Ph.D. dissertation, Department of Statistics, Rutgers University, Piscataway, NJ, Mar. 2004, thesis advisor: Professor Lawrence A. Shepp.

[29] M. Y. Vardi, L. Shepp, and L. Kaufman, "A statistical model for positron emission tomography," *Journal of the American Statistical Association*, vol. 80, no. 389, pp. 8–20, Mar. 1985.

[30] M. Beil, F. Fleischer, S. Paschke, and V. Schmidt, "Statistical analysis of 3D centromeric heterochromatin structure in interphase nuclei," *Journal of Microscopy*, vol. 217, pp. 60–68, 2005.

[31] D. L. Snyder, "Filtering and detection for doubly stochastic Poisson processes," *IEEE Trans. Inf. Theory*, vol. 18, no. 1, pp. 91–102, Jan. 1972.

[32] J. R. Pierce, "Optical channels: practical limits with photon-counting," *IEEE Trans. Inf. Theory*, vol. 26, no. 12, pp. 1819–1821, Dec. 1978.

[33] J. R. Pierce, E. C. Posner, and E. R. Rodemich, "The capacity of the photon counting channel," *IEEE Trans. Inf. Theory*, vol. 27, no. 1, pp. 61–77, Jan. 1981.

[34] J. L. Massey, "Capacity cutoff rate, and coding for direct detection optical channel," *IEEE Trans. Commun.*, vol. 29, no. 11, pp. 1615–1621, Nov. 1981.

[35] E. S. Sousa, "Performance of a spread spectrum packet radio network link in a Poisson field of interferers," *IEEE Trans. Inf. Theory*, vol. 38, no. 6, pp. 1743–1754, Dec. 1992.

[36] J. Ilow, D. Hatzinakos, and A. N. Venetsanopoulos, "Performance of FH SS radio networks with interference modeled as a mixture of Gaussian and alpha-stable noise," *IEEE Trans. Commun.*, vol. 46, no. 4, pp. 509–520, Apr. 1998.

[37] C. C. Chan and S. V. Hanly, "Calculating the outage probability in a CDMA network with spatial Poisson traffic," *IEEE Trans. Veh. Technol.*, vol. 50, no. 1, pp. 183–204, Jan. 2001.

[38] F. Baccelli, B. Błaszczyszyn, and F. Tournois, "Spatial averages of coverage characteristics in large CDMA networks," *Wireless Networks*, vol. 8, no. 6, pp. 569–586, Nov. 2002.

[39] X. Yang and A. P. Petropulu, "Co-channel interference modeling and analysis in a Poisson field of interferers in wireless communications," *IEEE Trans. Signal Process.*, vol. 51, no. 1, pp. 64–76, 2003.
[40] J. Orriss and S. K. Barton, "Probability distributions for the number of radio transceivers which can communicate with one another," *IEEE Trans. Commun.*, vol. 51, no. 4, pp. 676–681, Apr. 2003.
[41] S. P. Weber, X. Yang, J. G. Andrews, and G. de Veciana, "Transmission capacity of wireless ad hoc networks with outage constraints," *IEEE Trans. Inf. Theory*, vol. 51, no. 12, pp. 4091–4102, Dec. 2005.
[42] O. Dousse, F. Baccelli, and P. Thiran, "Impact of interferences on connectivity in ad hoc networks," *IEEE/ACM Trans. Netw.*, vol. 13, no. 2, pp. 425–436, Apr. 2005.
[43] O. Dousse, M. Franceschetti, and P. Thiran, "On the throughput scaling of wireless relay networks," *IEEE Trans. Inf. Theory*, vol. 52, no. 6, pp. 2756–2761, Jun. 2006.
[44] L. Song and D. Hatzinakos, "Cooperative transmission in Poisson distributed wireless sensor networks: Protocol and outage probability," *IEEE Trans. Wireless Commun.*, vol. 5, no. 10, pp. 2834–2843, Oct. 2006.
[45] A. Ghasemi and E. S. Sousa, "Interference aggregation in spectrum-sensing cognitive wireless networks," *IEEE J. Sel. Topics Signal Process.*, vol. 2, no. 1, pp. 41–56, Feb. 2008.
[46] R. Menon, R. M. Buehrer, and J. H. Reed, "On the impact of dynamic spectrum sharing techniques on legacy radio systems," *IEEE Trans. Wireless Commun.*, vol. 7, no. 11, pp. 4198–4207, Nov. 2008.
[47] W. Ren, Q. Zhao, and A. Swami, "Power control in spectrum overlay networks: How to cross a multi-lane highway," *IEEE J. Sel. Areas Commun.*, vol. 27, no. 7, pp. 1283–1296, Sep. 2009.
[48] E. Salbaroli and A. Zanella, "Interference analysis in a Poisson field of nodes of finite area," *IEEE Trans. Veh. Technol.*, vol. 58, no. 4, pp. 1776–1783, May 2009.
[49] H. Inaltekin, M. Chiang, H. V. Poor, and S. B. Wicker, "The behavior of unbounded path-loss models and the effect of singularity on computed network characteristics," *IEEE J. Sel. Areas Commun.*, vol. 27, no. 7, pp. 1078–1092, Sep. 2009.
[50] R. K. Ganti and M. Haenggi, "Interference and outage in clustered wireless ad hoc networks," *IEEE Trans. Inf. Theory*, vol. 55, no. 9, pp. 4067–4086, Sep. 2009.
[51] F. Baccelli, B. Błaszczyszyn, and P. Mühlethaler, "Stochastic analysis of spatial and opportunistic Aloha," *IEEE J. Sel. Areas Commun.*, vol. 27, no. 7, pp. 1105–1119, Sep. 2009.
[52] V. Chandrasekhar and J. G. Andrews, "Uplink capacity and interference avoidance for two-tier femtocell networks," *IEEE Trans. Wireless Commun.*, vol. 8, no. 7, pp. 3498–3509, Jul. 2009.
[53] Q. Zhao, L. Tong, A. Swami, and Y. Chen, "Decentralized cognitive MAC for opportunistic spectrum access in ad hoc networks: A POMDP framework," *IEEE J. Sel. Areas Commun.*, vol. 25, no. 3, pp. 589–600, Apr. 2007.
[54] O. Simeone, I. Stanojev, S. Savazzi, Y. Bar-Ness, U. Spagnolini, and R. Pickholtz, "Spectrum leasing to cooperating secondary ad hoc networks," *IEEE J. Sel. Areas Commun.*, vol. 26, no. 1, pp. 203–213, Jan. 2008.
[55] L. C. Wang and A. Chen, "Effects of location awareness on concurrent transmissions for cognitive ad hoc networks overlaying infrastructure-based systems," *IEEE Trans. Mobile Comput.*, vol. 8, no. 5, pp. 577–589, May 2009.
[56] ECC, "Technical requirements for UWB DAA (detect and avoid) devices to ensure the protection of radiolocation services in the bands 3.1 - 3.4 GHz and 8.5 - 9 GHz and BWA terminals in the band 3.4 - 4.2 GHz," 2008.
[57] G. Samoradnitsky and M. Taqqu, *Stable Non-Gaussian Random Processes*. Chapman and Hall, 1994.
[58] R. K. Ganti and M. Haenggi, "Interference in ad hoc networks with general motion-invariant node distributions," in *Proc. IEEE Int. Symp. on Inf. Theory*, Toronto, CANADA, Jul. 2008, pp. 1–5.
[59] P. Carr, H. Geman, D. B. Madan, and M. Yor, "The fine structure of asset returns: An empirical investigation," *The Journal of Business*, vol. 75, no. 2, pp. 305–332, Apr. 2002.
[60] N. Bambos and S. Kandukuri, "Power controlled multiple access (PCMA) schemes for next-generation wireless packet networks," *IEEE Trans. Wireless Commun.*, vol. 9, no. 3, pp. 58–64, Mar. 2002.
[61] G. J. Foschini and Z. Miljanic, "A simple distributed autonomous power control algorithm and its convergence," *IEEE Trans. Veh. Technol.*, vol. 42, no. 4, pp. 641–646, Nov. 1993.
[62] V. Chandrasekhar, J. G. Andrews, and A. Gatherer, "Femtocell networks: A survey," *IEEE Commun. Mag.*, vol. 46, no. 9, pp. 59–67, Sep. 2008.
[63] J. Gil-Pelaez, "Note on the inversion theorem," *Biometrika*, vol. 38, no. 3/4, pp. 481–482, Dec. 1951.

Alberto Rabbachin (S'03–M'07) received the M.S. degree from the University of Bologna (Italy) in 2001 and the Ph.D. degree from the University of Oulu (Finland) in 2008.

Since 2008 he is a Postdoctoral researcher with the Institute for the Protection and Security of the Citizen of the European Commission Joint Research Center. He has done research on ultrawideband (UWB) impulse-radio techniques, with emphasis on receiver architectures, synchronization, and ranging algorithms, as well as on low-complexity UWB transceiver design. He is the author of several book chapters, international journal papers, conference proceedings, and international standard contributions. His current research interests include aggregate interference statistical modeling, cognitive radio, and wireless body area networks. Dr. Rabbachin received the Nokia Fellowship for year 2005 and 2006, the IEEE Globecom 2010 Best Paper Award, the IEEE Globecom 2010 GOLD Best Paper Award, and the European Commission JRC Best Young Scientist Award 2010. He has served on the Technical Program Committees of various international conferences.

Tony Q.S. Quek (S'98–M'08) received the B.E. and M.E. degrees in Electrical and Electronics Engineering from Tokyo Institute of Technology, Tokyo, Japan, in 1998 and 2000, respectively. At Massachusetts Institute of Technology (MIT), Cambridge, MA, he earned the Ph.D. in Electrical Engineering and Computer Science in Feb. 2008.

Since 2008, he has been with the Institute for Infocomm Research, A*STAR, where he is currently a Principal Investigator and Senior Research Engineer. He is also an Adjunct Assistant Professor with the Division of Communication Engineering, Nanyang Technological University. His main research interests are the application of mathematical, optimization, and statistical theories to communication, detection, information theoretic and resource allocation problems. Specific current research topics include cooperative networks, interference networks, heterogeneous networks, green communications, wireless security, and cognitive radio.

Dr. Quek has been actively involved in organizing and chairing sessions, and has served as a member of the Technical Program Committee (TPC) in a number of international conferences. He served as the Technical Program Chair for the Services & Applications Track for the IEEE Wireless Communications and Networking Conference (WCNC) in 2009, the Cognitive Radio & Cooperative Communications Track for the IEEE Vehicular Technology Conference (VTC) in Spring 2011, and the Wireless Communications Symposium for the IEEE Globecom in 2011; as Technical Program Vice-Chair for the IEEE Conference on Ultra Wideband in 2011; and as the Workshop Chair for the IEEE Globecom 2010 Workshop on Femtocell Networks and the IEEE ICC 2011 Workshop on Heterogeneous Networks. Dr. Quek is currently an Editor for WILEY JOURNAL ON SECURITY AND COMMUNICATION NETWORKS. He was Guest Editor for the JOURNAL OF COMMUNICATIONS AND NETWORKS (Special Issue on Heterogeneous Networks) in 2011.

Dr. Quek received the Singapore Government Scholarship in 1993, Tokyu Foundation Fellowship in 1998, and the A*STAR National Science Scholarship in 2002. He was honored with the 2008 Philip Yeo Prize for Outstanding Achievement in Research and the IEEE Globecom 2010 Best Paper Award.

Hyundong Shin (S'01–M'04) received the B.S. degree in Electronics Engineering from Kyung Hee University, Korea, in 1999, and the M.S. and Ph.D. degrees in Electrical Engineering from Seoul National University, Seoul, Korea, in 2001 and 2004, respectively.

From September 2004 to February 2006, Dr. Shin was a Postdoctoral Associate at the Laboratory for Information and Decision Systems (LIDS), Massachusetts Institute of Technology (MIT), Cambridge, MA, USA. In March 2006, he joined the faculty of the School of Electronics and Information, Kyung Hee University, Korea, where he is now an Assistant Professor at the Department of Electronics and Radio Engineering. His research interests include wireless communications, information and coding theory, cooperative/ collaborative communications, and multiple-antenna wireless communication systems and networks.

Professor Shin served as a member of the Technical Program Committee in the IEEE International Conference on Communications (2006, 2009), the IEEE International Conference on Ultra Wideband (2006), the IEEE Global Communications Conference (2009, 2010), the IEEE Vehicular Technology Conference (2009 Fall, 2010 Spring, 2010 Fall), the IEEE International Symposium on Personal, Indoor and Mobile Communications (2009, 2010), and the IEEE Wireless Communications and Networking Conference (2010). He served as a Technical Program co-chair for the IEEE Wireless Communications and Networking Conference PHY Track (2009). Dr. Shin is currently an Editor for the IEEE TRANSACTIONS ON WIRELESS COMMUNICATIONS and the KSII Transactions on Internet and Information Systems. He was a Guest Editor for the 2008 EURASIP Journal on Advances in Signal Processing (Special Issue on Wireless Cooperative Networks).

Professor Shin received the IEEE Communications Society's Guglielmo Marconi Best Paper Award (2008) and the IEEE Vehicular Technology Conference Best Paper Award (2008 Spring).

Moe Z. Win (S'85-M'87-SM'97-F'04) received both the Ph.D. in Electrical Engineering and M.S. in Applied Mathematics as a Presidential Fellow at the University of Southern California (USC) in 1998. He received an M.S. in Electrical Engineering from USC in 1989, and a B.S. (*magna cum laude*) in Electrical Engineering from Texas A&M University in 1987.

Dr. Win is an Associate Professor at the Massachusetts Institute of Technology (MIT). Prior to joining MIT, he was at AT&T Research Laboratories for five years and at the Jet Propulsion Laboratory for seven years. His research encompasses developing fundamental theories, designing algorithms, and conducting experimentation for a broad range of real-world problems. His current research topics include location-aware networks, intrinsically secure wireless networks, aggregate interference in heterogeneous networks, ultra-wide bandwidth systems, multiple antenna systems, time-varying channels, optical transmission systems, and space communications systems.

Professor Win is an IEEE Distinguished Lecturer and elected Fellow of the IEEE, cited for "contributions to wideband wireless transmission." He was honored with two IEEE technical field awards: the IEEE Kiyo Tomiyasu Award (2011) for "fundamental contributions to high-speed reliable communications over optical and wireless channels" and the IEEE Eric E. Sumner Award (2006, jointly with R.A. Scholtz) for "pioneering contributions to ultra-wide band communications science and technology." Together with students and colleagues, his papers have received several awards including the IEEE Communications Society's Guglielmo Marconi Best Paper Award (2008) and the IEEE Antennas and Propagation Society's Sergei A. Schelkunoff Transactions Prize Paper Award (2003). His other recognitions include the Outstanding Service Award of the IEEE ComSoc Radio Communications Committee (2010), the Laurea Honoris Causa from the University of Ferrara, Italy (2008), the Technical Recognition Award of the IEEE ComSoc Radio Communications Committee (2008), Wireless Educator of the Year Award (2007), the Fulbright Foundation Senior Scholar Lecturing and Research Fellowship (2004), the U.S. Presidential Early Career Award for Scientists and Engineers (2004), the AIAA Young Aerospace Engineer of the Year (2004), and the Office of Naval Research Young Investigator Award (2003).

Professor Win has been actively involved in organizing and chairing a number of international conferences. He served as the Technical Program Chair for the IEEE Wireless Communications and Networking Conference in 2009, the IEEE Conference on Ultra Wideband in 2006, the IEEE Communication Theory Symposia of ICC-2004 and Globecom-2000, and the IEEE Conference on Ultra Wideband Systems and Technologies in 2002; Technical Program Vice-Chair for the IEEE International Conference on Communications in 2002; and the Tutorial Chair for ICC-2009 and the IEEE Semiannual International Vehicular Technology Conference in Fall 2001. He is an elected Member-at-Large on the IEEE Communications Society Board of Governors (2011-2013). He was the chair (2004-2006) and secretary (2002-2004) for the Radio Communications Committee of the IEEE Communications Society. Dr. Win is currently an Editor for IEEE TRANSACTIONS ON WIRELESS COMMUNICATIONS. He served as Area Editor for *Modulation and Signal Design* (2003-2006), Editor for *Wideband Wireless and Diversity* (2003-2006), and Editor for *Equalization and Diversity* (1998-2003), all for the IEEE TRANSACTIONS ON COMMUNICATIONS. He was Guest-Editor for the PROCEEDINGS OF THE IEEE (Special Issue on UWB Technology & Emerging Applications) in 2009 and IEEE JOURNAL ON SELECTED AREAS IN COMMUNICATIONS (Special Issue on Ultra -Wideband Radio in Multiaccess Wireless Communications) in 2002.